

Surprise and recency in novelty detection in the primate brain

Highlights

- High channel count electrophysiology shed light on mechanisms of novelty detection
- Object novelty selectivity is intertwined with computations of recency and surprise
- Learning and across-day forgetting of novel objects occur at multiple timescales
- Learning and across-day forgetting are correlated across single neurons

Authors

Kaining Zhang,
Ethan S. Bromberg-Martin,
Fatih Sogukpinar, Kim Kocher,
Ilya E. Monosov

Correspondence

ilya.monosov@gmail.com

In brief

Zhang et al. show that novelty selectivity emerges intertwined with the computations of recency (how long ago a stimulus was experienced) and sensory surprise (violation of predictions about incoming stimuli). Learning and across-day forgetting of novel objects occur at multiple timescales and are correlated at the level of single neurons.



Article

Surprise and recency in novelty detection in the primate brain

Kaining Zhang,¹ Ethan S. Bromberg-Martin,² Fatih Sogukpinar,³ Kim Kocher,² and Ilya E. Monosov^{1,2,3,4,5,6,*}

¹Department of Biomedical Engineering, Washington University, St. Louis, MO 63130, USA

²Department of Neuroscience, Washington University School of Medicine, St. Louis, MO 63110, USA

³Department of Electrical Engineering, Washington University, St. Louis, MO 63130, USA

⁴Department of Neurosurgery School of Medicine, Washington University, St. Louis, MO 63110, USA

⁵Pain Center, Washington University School of Medicine, St. Louis, MO 63110, USA

⁶Lead contact

*Correspondence: ilya.monosov@gmail.com

<https://doi.org/10.1016/j.cub.2022.03.064>

SUMMARY

Primates and other animals must detect novel objects. However, the neuronal mechanisms of novelty detection remain unclear. Prominent theories propose that visual object novelty is either derived from the computation of recency (how long ago a stimulus was experienced) or is a form of sensory surprise (stimulus unpredictability). Here, we use high-channel electrophysiology in primates to show that in many primate prefrontal, temporal, and subcortical brain areas, object novelty detection is intertwined with the computations of recency and sensory surprise. Also, distinct circuits could be engaged by expected versus unexpected sensory surprise. Finally, we studied neuronal novelty-to-familiarity transformations during learning across many days. We found a diversity of timescales in neurons' learning rates and between-session forgetting rates, both within and across brain areas, that are well suited to support flexible behavior and learning in response to novelty. Our findings show that novelty sensitivity arises on multiple timescales across single neurons due to diverse but related computations of sensory surprise and recency and shed light on the computational underpinnings of novelty detection in the primate brain.

INTRODUCTION

Humans and other primates learn from the world by exploring objects. Behavioral experiments in primates show that novel visual objects—that is, objects they have never seen before—motivate behavior, by capturing attention and gaze and promoting the formation of new memories.^{1–10} Yet despite the importance of novel objects in our daily life, we currently lack an understanding of how novelty selectivity arises in primate brain circuits and lack an algorithmic understanding of biological novelty detection.

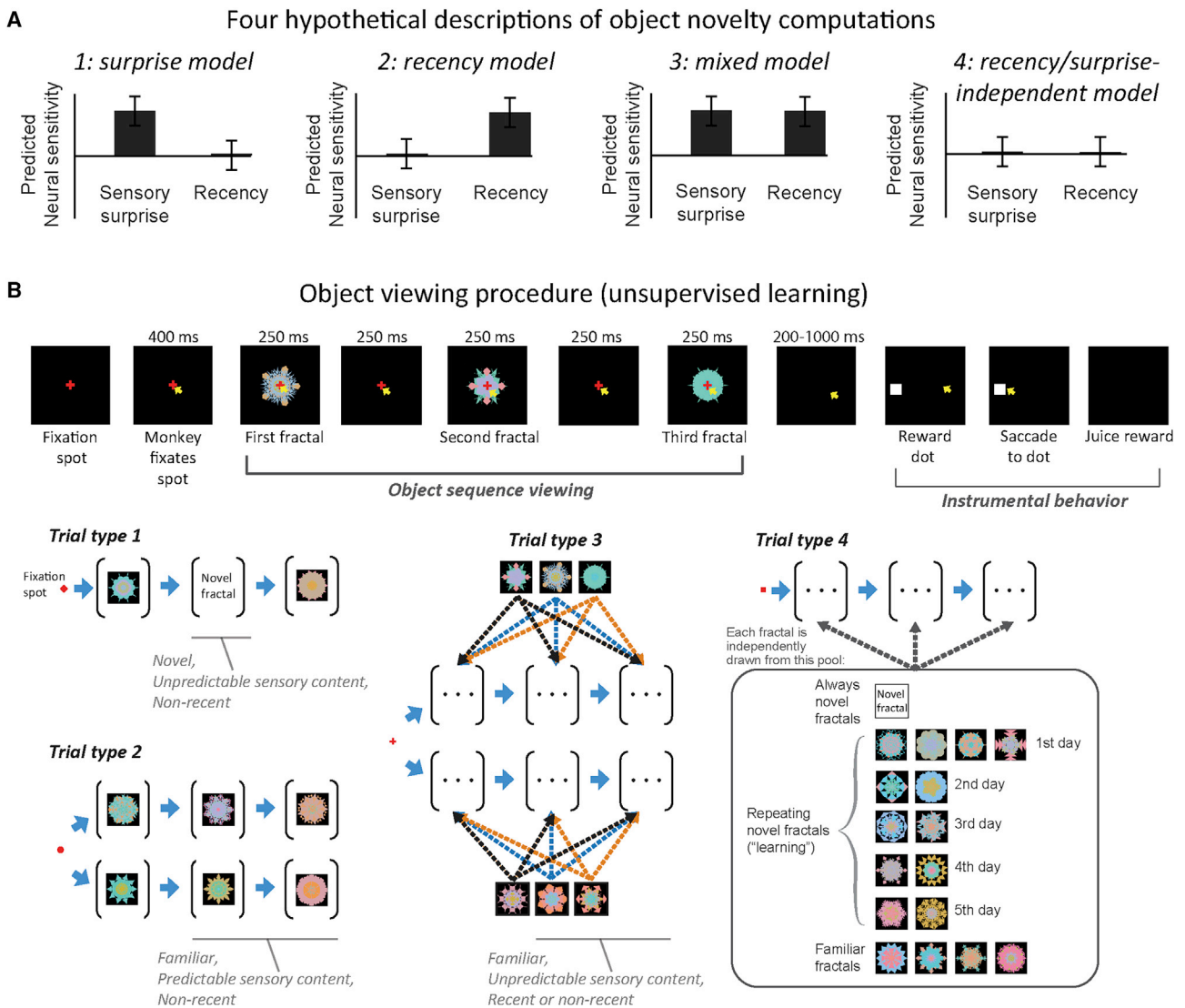
Previous studies reported that neurons in many primate brain areas are novelty responsive—that is, they respond differently to novel versus familiar stimuli.^{3,11–14} However, novel stimuli differ from familiar stimuli in many respects. For instance, novel stimuli are unexpected or surprising, deviate from recent experiences, and motivate behavior.^{14–20} Such broad and diverse properties of perceptual novelty not only highlight that it is critical to understand the neural mechanisms of novelty detection but also illustrate why it has been challenging to dissociate representations of novelty from other neural signals, particularly in higher order brain areas.

There are several formal theories and hypothesized algorithms for processing and detecting perceptual novelty that each suggest related but dissociable mechanisms for novelty detection. They make distinct predictions about the nature of

novelty-responsive neurons in the brain (Figure 1A). The first one conceptualizes novelty as a form of sensory surprise^{13,18,20–25} (Figure 1A, Model 1). Sensory surprise is a violation of predictions about incoming sensory information and could be due to the probability of a specific stimulus or the overall sensory statistics of a given context, such as when expected sequences of objects are violated.^{3,18} In this conception, novelty-responsive neurons ought to be sensitive to sensory surprises due to errors in prediction about which sensory events occur. A second class of models conceptualize novelty as a recency and/or repetition effect, which is commonly operationally defined as a neural or behavioral sensitivity to how long ago a stimulus was experienced^{8,9,26–28} (Figure 1A, Model 2). While these two processes could be distinct, these processes could also be interdependent and cooperate,^{9,29} particularly if the brain contains circuits with multiple timescales of object memory. Hence, it is possible that novelty selectivity could arise with both sensory surprise and recency computations (Model 3) or that each contributes to novelty computations preferentially in different brain areas. Finally, novelty responses could arise independently of sensory surprise or recency, as a categorical signal for complete novelty that purely indicates whether or not a stimulus has ever been seen before (Model 4).^{18,19,30}

We set out to (1) test the relationship between novelty, recency, and different forms of sensory surprise and (2) explore





the nature and timescales of novelty representations in the activity of single neurons. To do this, we implanted two monkeys with semi-chronic high channel count arrays and recorded neurons across temporal cortex, amygdala, hippocampus, basal ganglia, and the prefrontal cortices while monkeys participated in unsupervised learning object viewing procedures that assessed the relationship of single neurons' object novelty responses with recency and sensory surprise.

Our findings show that object novelty sensitivity is heavily intertwined with computations of several forms of sensory surprise and recency in single neurons and operates over diverse timescales both within and across brain areas. These data shed light on the logic and computational underpinnings of novelty detection in the primate brain.

RESULTS

Measuring novelty, recency, and surprise

On each trial, the monkey was shown a sequence of three fractal visual objects. The objects in these sequences did not possess instrumental value and did not affect reward rate or magnitude (STAR Methods). Monkeys obtained reward after successfully observing each object sequence and then participating in a distinct instrumental behavior that consisted of making an eye movement to a dot that appeared at one of four possible locations on the screen (Figure 1B, top right).

To observe the relationship of novelty with sensory surprise and recency, this procedure contained several trial types that included distinct object sequences designed to dissociate these

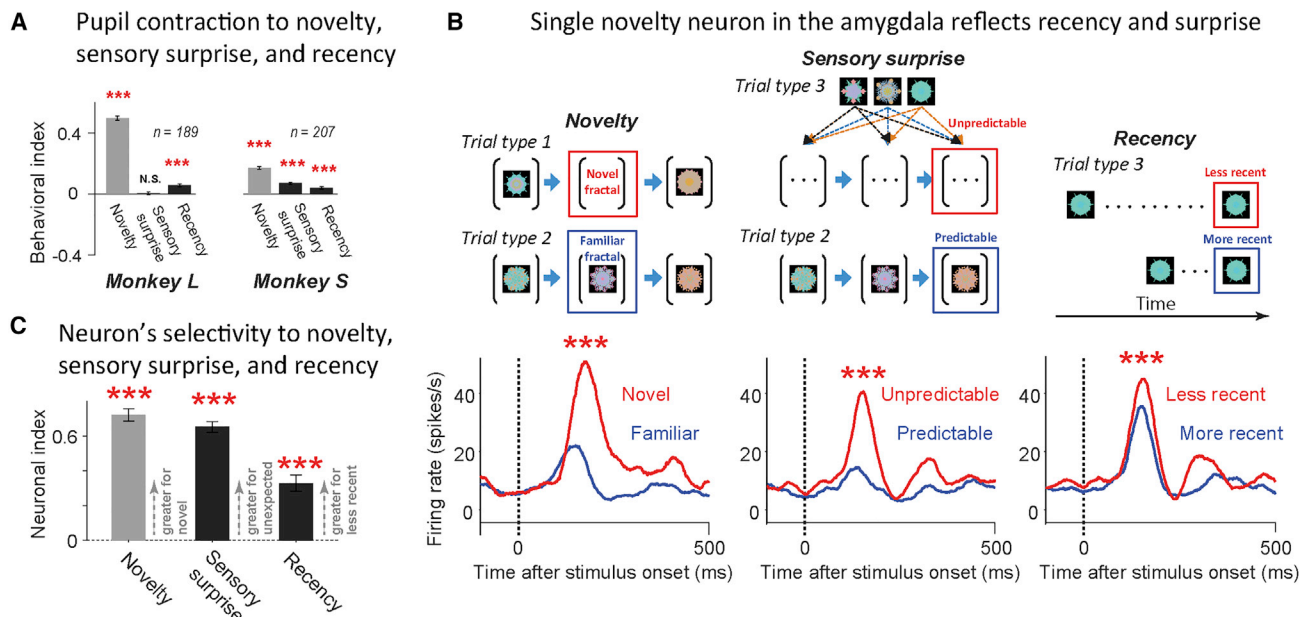


Figure 2. Pupillary and neural signatures of novelty coding

(A) Pupillary responses of monkeys L and S. Error bars are SE.

(B) A single neuron in the amygdala is sensitive to novelty, sensory surprise, and recency. PSTHs were smoothed using a Gaussian kernel (SD = 50 ms).

(C) Sensitivity indices based on the activity in (B). *** $p < 0.001$, error bar indicates bootstrap SE. The derivation of the indices is detailed in STAR Methods and conceptually shown by the cartoon in (B). Blue and red boxes in the cartoon mark the conditions corresponding to the spike density functions in (B) that were used to derive the sensitivity indices.

Control analyses for this figure are shown in Figures S1 and S2.

factors (STAR Methods). The trial type was cued to the animal at the start of the trial by the shape of the fixation point (Figure 1). In Type 1 trials, the monkeys experienced a sequential presentation of three objects, in which the second object was always novel, and the other objects were familiar and fully predictable (Figure 1B). The novel objects had never been seen before because they were generated on a trial by trial basis using a new random seed on each trial (using a previously established algorithm).^{3,14,31–33} In Type 2 trials, monkeys experienced other distinct fractal visual objects that were all highly familiar. For these trials, we used two sets of objects to control for single neurons' object sensitivities (Figure 1B; STAR Methods), and following the presentation of the first fractal, the remaining objects in the sequence were predictable (Figure 1B). Hence, the variability or entropy of which object would be presented was relatively low. We defined novelty-responsive neurons as those that responded differentially to the second objects in Type 1 versus Type 2 trials.³ Importantly, this design ensured that it was highly predictable whether the second object in these sequences would be novel or familiar, so that neural novelty responses could not be attributed to the novelty simply being more unpredictable or surprising than familiarity.

During the same recording session, we also measured neuronal sensitivities to object recency and sensory surprise. This was accomplished with Type 3 trials that contained three objects that were each drawn from a familiar set of three fractals but were drawn in a random sequence with replacement (Figure 1B). Thus, following the presentation of the first fractal in Type 3 trials, the monkey could predict which set of fractals

the remaining two objects would be drawn from, but could not fully predict their specific object identities. Hence, variability or entropy of which object would be presented was relatively high. By comparing Type 2 and Type 3 trials, we measured neural sensitivity to sensory surprise—that is, responses that were attributable to the presentation of an object whose identity and sensory features were predictable versus unpredictable. Furthermore, neural sensitivity to recency was assessed by comparing responses to familiar objects during Type 3 trials that were more or less recently seen (Figure 1B; STAR Methods; Xiang et al.⁸). Hence, from Type 1–3 trials, we obtained measures of each neuron's sensitivity to novelty, surprise, and recency. Importantly, these measurements were independent of each other (STAR Methods). Thus, any relationship between these measures reflects a relationship between how neurons generate their responses to these variables (such as is hypothesized by the models in Figure 1A). We also used a distinct set of trials to study learning and the timescales of novelty-to-familiarity transformations (Type 4; we return to them later).

Because we used an unsupervised object viewing procedure that required the monkeys to fixate during object sequences, we were also able to measure pupillary responses to novelty, recency, and sensory surprise. Both animals were sensitive to the task because their pupillary constrictions reliably changed as a function of all or most of these variables (Figure 2A; Monkey L: novelty index, $p < 0.0001$; sensory surprise index, $p < 0.0001$; recency index, $p < 0.0001$; Monkey S: novelty index, $p < 0.0001$; sensory surprise index, $p = 0.57$; recency index, $p < 0.0001$). Constriction of pupils to expected novel stimuli replicated

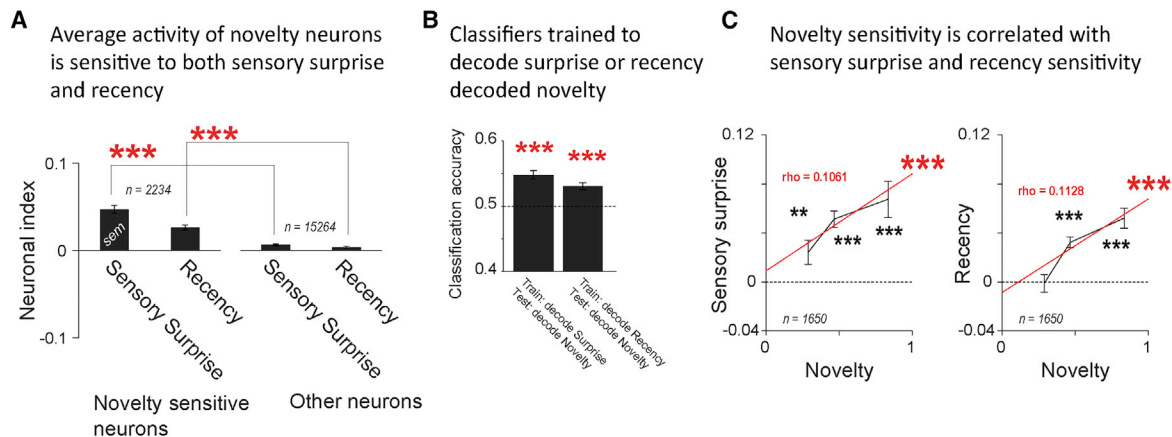


Figure 3. Novelty neurons are sensitive to sensory surprise and recency

(A) Novelty-responsive neurons displayed particularly strong sensitivity to sensory surprise and recency. Population mean sensory surprise and recency indices are shown for novelty-responsive neurons (left) and all other neurons (right). Error bars in all panels are SE. ** $p < 0.01$, *** $p < 0.001$. (B) Two classifiers' performance (left and right) at classifying objects as novel versus familiar. These classifiers were trained on responses to familiar fractals to discriminate sensory-surprising versus predictable fractals (left) and recent versus non-recent fractals (right). (C) The magnitude of novelty-excited neurons' novelty sensitivity was correlated with the magnitude of their sensitivity to sensory surprise (left) and recency (right). Control analyses for this figure are shown in [Figures S1](#) and [S2](#).

previous human data.^{34–36} Also, monkeys had faster reaction times to initiate Type 1 trials, which contained a novel fractal, than Type 2 trials ([Figure S1A](#); Type 1 versus Type 2, $p = 0.00014$). This novelty seeking behavior is consistent with previous findings.¹⁴ Monkeys also had faster reaction times to initiate Type 3 trials, which contained objects that were less predictable than Type 2 trials (Type 2 versus Type 3, $p < 0.0001$).

In our neuronal data, we uncovered a clear relationship between the encoding of novelty and surprise and recency, consistent with Model 3 ([Figures 2B](#) and [2C](#)). An example neuron recorded in the amygdala is shown in [Figure 2B](#). This neuron discriminated novel from familiar objects, displaying greater excitation to predicted novel objects than to predicted familiar objects ([Figure 2B](#), left). The neuron was also sensitive to surprise: it was relatively more excited by unpredicted versus predicted familiar stimuli ([Figure 2B](#), middle). Also, this neuron was sensitive to recency: it was more excited by objects that were presented relatively less recently ([Figure 2B](#), right). Therefore, the cell was selectively excited by all three types of objects—novel, surprising, and less-recent objects. We quantified this result by computing an index of each neuron's sensitivity for each of these types of objects ([Figure 2C](#); [STAR Methods](#)). Indices >0 indicate a preference for novelty, sensory surprise, or less-recent objects respectively. This pattern resembled Model 3 ([Figure 1A](#)).

A similar result emerged at the population level ($n = 2,234$ novelty-responsive neurons). Novelty-responsive neurons displayed significant sensitivity to sensory surprise and recency (mean of sensory surprise index = 0.0468, mean of recency index = 0.0263, both greater than 0, $p < 0.0001$, signed-rank tests; [Figure 3A](#)). Crucially, those effects were much greater in novelty neurons versus all other recorded neurons ([Figure 3A](#); $p < 0.0001$, rank-sum test; [Figure S1](#) for each animal). We also found that object novelty could be decoded based on neural tuning to surprise and recency. We trained a classifier on all neurons in each session to decode whether the fractals were sensory

surprising, and another classifier to decode whether the fractals were nonrecent. The two classifiers were both able to decode object novelty significantly above chance ([Figure 3B](#), [S1D](#), and [S1E](#); sensory surprise and recency classifiers, both $p < 0.0001$). Moreover, on a neuron-by-neuron level, for novelty-excited neurons, the magnitude of sensitivity to novelty was correlated with the magnitude of sensitivity to sensory surprise ([Figure 3C](#), left) and recency ([Figure 3C](#), right; [Figure S2](#)). Furthermore, these effects were not produced by other factors such as object selectivity, sequence position effects, or any potential statistical dependencies between the indexes ([Figure S2](#)).

Novelty, recency, and surprise are related across brain regions

Novelty sensitivity was not uniformly distributed throughout single neurons in the primate brain. Some brain areas, in particular the anterior ventral medial temporal cortex (AVMTC), and areas that it is interconnected with, such as area 46v, basal forebrain, and the amygdala, were preferentially enriched in novelty-responsive neurons ([Figure 4A](#)). Consistent with [Figures 3A–3C](#), we found that there was an across-region relationship between novelty, recency, and sensory surprise—that is, on average, regions that were preferentially enriched with novelty-responsive neurons were also enriched with neurons that were responsive to recency and sensory surprise (significantly higher percentage of sensory surprise responsive neurons [$p < 0.0001$, permutation test] and recency responsive neurons [$p < 0.0001$, permutation test] when comparing the 1/5th of areas with the highest percentage of novelty-responsive neurons to the 1/5th of areas with the lowest percentage of novelty-responsive neurons; [Figure 4A](#), left).

This finding raised the question of whether the relationship between novelty and sensory surprise and recency is only relevant to a small number of brain areas that are most enriched with novelty-responsive neurons, or whether this relationship is a general

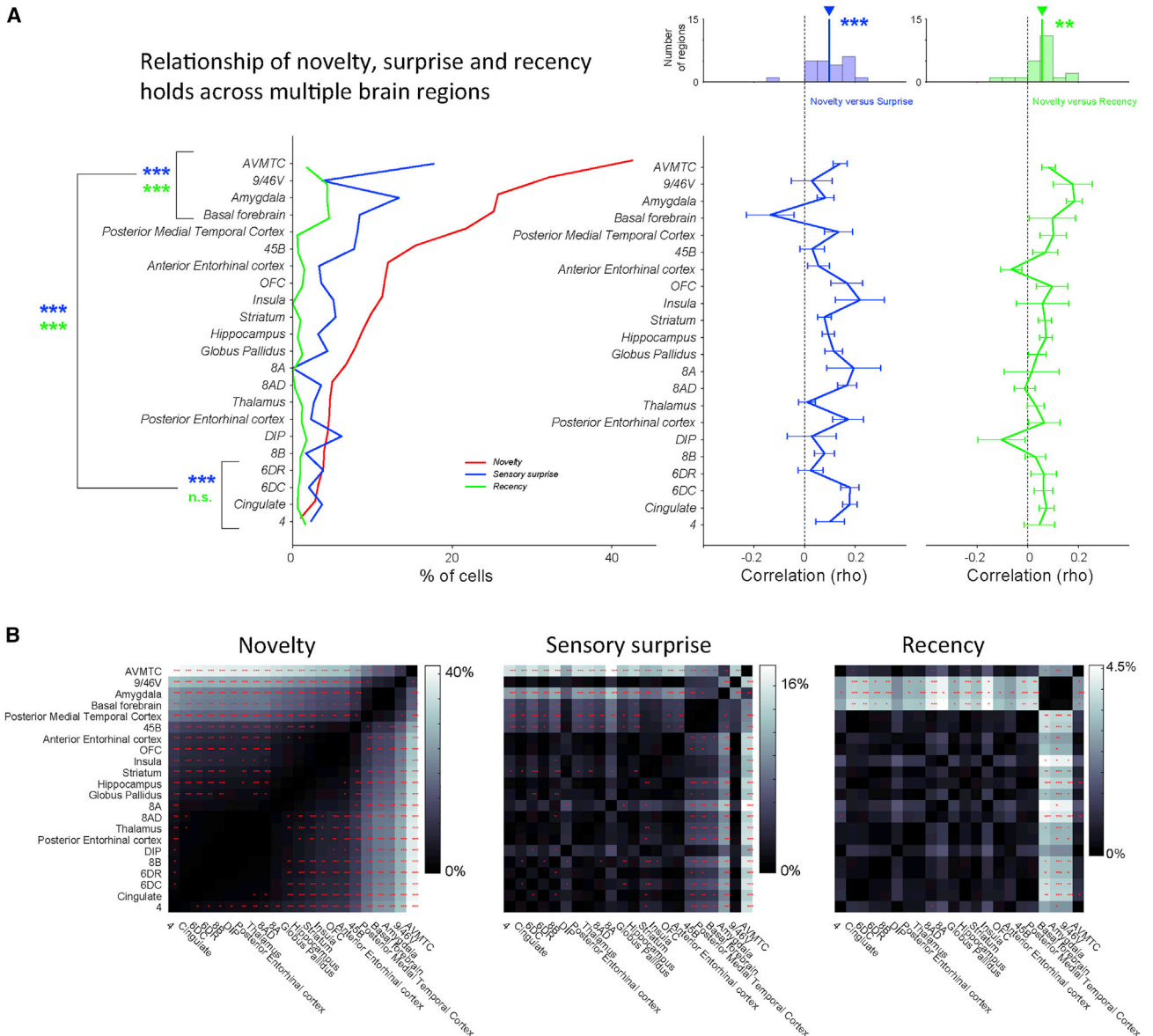


Figure 4. Novelty neuron sensitivities to sensory surprise and recency in different brain regions

(A) Novelty, sensory surprise, and recency computations often co-occur across the brain. Percent of neurons significantly responsive to novelty (red), sensory surprise (blue), and recency (green) shown across brain areas that were rank ordered by the percentage of neurons responsive to novelty (left; x axis). The top four brain areas had more neurons than would be expected by chance that were responsive to recency and surprise (colored asterisks, binomial test) and significantly more than the bottom four areas ($p < 0.0001$, permutation test). Within the brain areas, novelty versus sensory surprise (middle) and novelty versus recency (right) are positively correlated in most areas (top histograms, signed-rank test relative to 0, $**p < 0.01$, $***p < 0.001$). Error bars indicate SE obtained through a bootstrapping procedure. A more detailed visualization of these data is shown in [Figure S3](#).

(B) Pairwise comparison between brain areas of their percentage of novelty-responsive neurons (left), sensory surprise responsive neurons (middle), and recency responsive neurons (right). The colors in the matrix represent the absolute difference in percentages of responsive neurons, and the red asterisks indicate whether the differences are significant (Fisher's exact test, $*p < 0.05$, $**p < 0.01$, $***p < 0.001$). A summary of surprise signals from sequence violations is shown in [Figure S3](#). Additional population analyses of novelty neurons are in [Figure S5](#). Recording locations are reported in [Figure S7](#).

feature common to brain areas involved in novelty processing. Our data indicate that the latter is the case: there were remarkably consistent positive correlations between novelty and both sensory surprise and recency across almost all of the recorded brain areas ([Figure 4A](#), right). This suggests that the results in [Figure 3C](#) generalize across most brain areas that we targeted in this study. In sum, these data show that the novelty is linked

measurements of sensory surprise and recency in many brain areas.

This finding also raised the question of whether novelty processing is linked to other types of sensory surprises as well. For example, we recently showed that novelty-responsive neurons in the basal forebrain are sensitive to violations in highly over trained object sequences, responding when a familiar

object from one sequence unexpectedly appears in another.³ To replicate this and test whether it holds across the many brain areas recorded here, we introduced object sequence violations on a small fraction of Type 2 trials (~10%) and computed an index that measured neural sensitivity to them (STAR Methods). By contrast to the sensory surprise index, which measures surprises that can be fully expected to occur, the violation index measures surprises that should be highly unexpected, as they are both low probability and violate the typical task structure. This produced a remarkably similar pattern of results: novelty-responsive neurons were significantly sensitive to sequence violations, and their sensitivity to novelty and sequence violations were positively correlated, particularly in the basal forebrain (Figure S3). This indicates that the results in Figures 3A and 3B can generalize to other types of sensory surprises and highlight the importance of the basal forebrain in novelty and surprise computations in the many brain regions that receive its projections.^{37,38}

Furthermore, the data show that expected surprise and unexpected surprise may sometimes engage distinct cells or circuits. For example, within the basal forebrain, novelty is positively correlated with sequence violations³ but negatively correlated with expected sensory surprises. Hence, basal forebrain neurons treat unexpected sequence violations differently from expected sensory surprises. Consistent with differences among expected and unexpected surprises at the level of neural circuits, some brain areas, such as the hippocampus and the striatum, were relatively more engaged by sequence violations than sensory surprises (Figure S3D).

Also, the fact that novelty, sensory surprise, and recency were not treated precisely identically across brain areas was highlighted by distance matrixes between brain areas based on their differences in the percentage of cells with significant coding of these variables (Figures 4B and S3). These three distance matrixes were highly correlated with each other, with the same cluster of 4–5 areas standing out from the rest (novelty versus recency, $\rho = 0.502$, $p < 0.0001$; novelty versus sensory surprise, $\rho = 0.585$, $p < 0.0001$; sensory surprise versus recency, $\rho = 0.327$, $p < 0.0001$, Spearman's rank correlation). However, within this group there were differences among brain areas as well. AVMTC was highly enriched in novelty and sensory surprise coding but less so in recency; 9/46v was enriched in novelty and recency but less so in sensory surprise, whereas amygdala and basal forebrain integrated all three. In addition, recency and surprise sensitivity were significantly positively correlated across all neurons ($\rho = 0.07$, $p < 0.001$; animal S, $\rho = 0.1154$, $p < 0.001$; animal L, $\rho = 0.025$, $p = 0.0255$) but not always across novelty-excited neurons ($\rho = 0.04$, $p = 0.0896$; animal S, $\rho = 0.25$, $p < 0.001$; animal L, $\rho = -0.125$, $p < 0.001$). Thus, our data suggest that specific subpopulations of novelty-responsive neurons can be especially sensitive to either surprise, recency, or both.

Arousal does not induce the relationship of novelty with recency and surprise

Next, we asked whether these correlated codes could have been induced not by common computations but by common changes in arousal in response to novelty, surprise, and recency.¹⁰ In our data, this was unlikely because while neural populations recorded in each monkey displayed similar patterns as Figure 3

(Figure S1), their pupillary responses to sensory surprise differed (Figure 2A), suggesting that the main population-level results could not be just a reflection of pupil-indexed arousal. To test this further, we recorded the activity of many of the same neurons while manipulating arousal in a reward information viewing procedure that measured how novelty-sensitive neurons anticipated and responded to information about future rewards. Here, monkeys observed objects that indicated changes in reward value and uncertainty (Figure 5A), which are known to strongly activate neural populations that regulate motivated behavior.^{39,40}

Our sampled neural populations were significantly enriched in neurons that were responsive to two important reward statistics known to drive arousal: (1) many neurons signaled reward values by discriminating high value from low value objects and (2) many neurons anticipated the receipt of information to resolve reward uncertainty by activating when reward was uncertain and increasing this activity before an informative cue would appear to indicate the reward outcome (Figure S4). Neuronal sensitivity to these two variables was not correlated with neuronal sensitivity to novelty, across the group of novelty-excited neurons (Figure 5B). This is consistent with a previous study that found a similar result using imaging (Ghazizadeh et al.;⁴¹ but note that in brain regions involved in controlling the deployment of spatial attention and gaze, they did find that there was indeed a relation between novelty and reward). The main point for this study is that in our data, on average, neuronal sensitivity to novelty was generally more strongly correlated with recency and with sensory surprise, than with reward value and with information anticipation (novelty and recency versus novelty and reward value, $p = 0.0008$; novelty and recency versus novelty and reward information, $p = 0.052$; novelty and sensory surprise versus novelty and reward value, $p = 0.0114$; novelty and sensory surprise versus novelty and reward information, $p = 0.276$; permutation tests). Neural coding indexes for sensory surprise and recency were not correlated with indexes for reward value and reward information anticipation at the population level (Figure 5C).

It is worth noting that novelty was unrelated to reward in our sequence task. Hence, these results do not shed light on the interaction between reward and novelty when novelty and reward covary within the same task, when the value of novel objects changes across trials, or when novelty signals the chance to learn the reward value of objects.^{42–44} Rather, the analyses fortify the notion that the population-wide results (Figures 3A–3C) were not simply due to task-induced fluctuations in object salience or arousal.

Compared with the more prevalent novelty-excited neurons, on average, novelty-inhibited neurons behaved slightly differently; they had marginally significant correlations with reward-related indices (Figure S4C), suggesting that they may have a different role in linking novelty, arousal, and reward processing.

Common origins of novelty responses

Next, we asked whether novelty responses share common origins across simultaneously recorded neurons. We found that during neural responses to objects, noise correlations were higher between pairs of novelty-responsive neurons than pairs of other neurons ($p = 0.002$, paired signed-rank test; Figure S5).

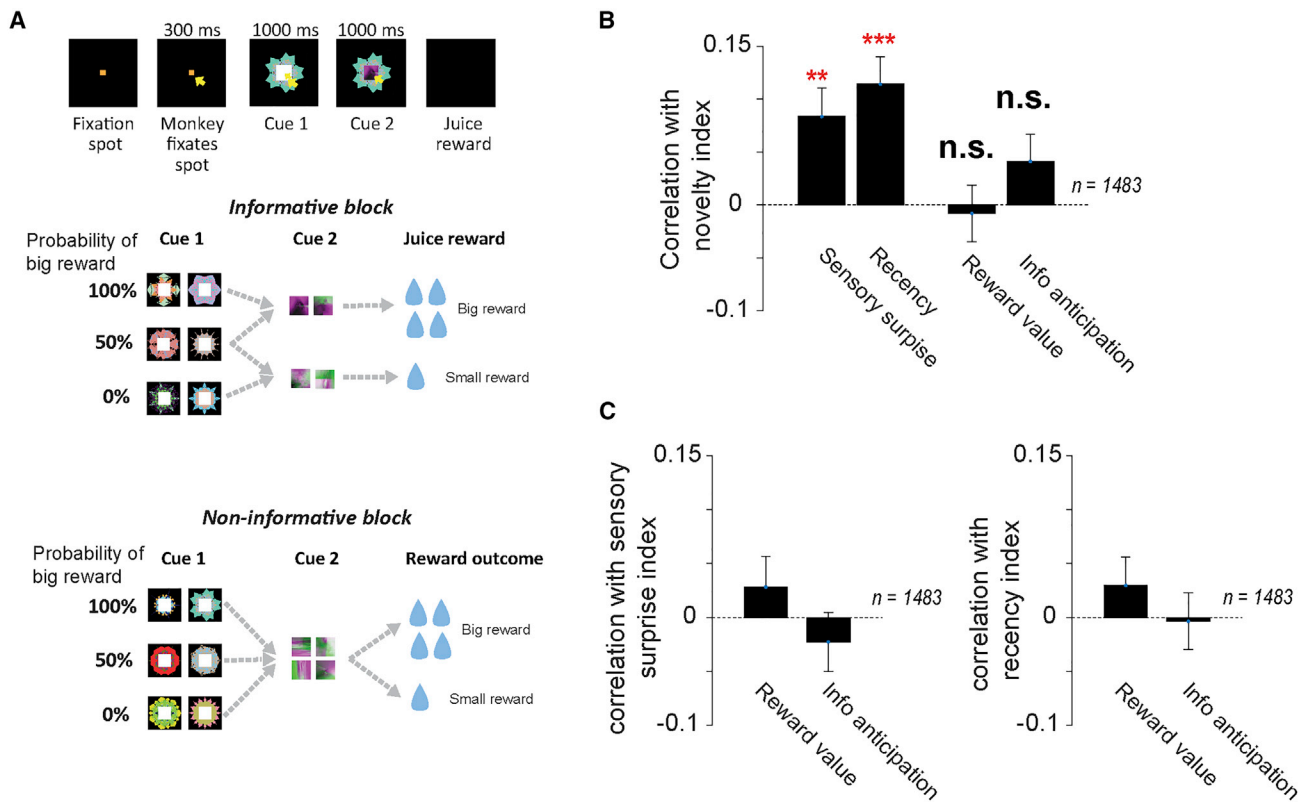


Figure 5. Neurons' excitatory responses to novelty in the object viewing procedure are on average not correlated with their responses in a distinct reward information viewing procedure

(A) Behavioral procedure for testing neural responses to changes in reward value and in anticipation of information to resolve reward uncertainty.

(B) Novelty-excited neurons' novelty sensitivity was not significantly correlated with their sensitivity to reward value and information anticipation (right two bars, $\rho = -0.0008$, $p = 0.76$, $\rho = 0.042$, $p = 0.11$), but was significantly correlated with their sensitivity to sensory surprise and recency (left two bars, $\rho = 0.084$, $p = 0.0013$, $\rho = 0.114$, $p < 0.0001$). * $p < 0.05$, ** $p < 0.01$, *** $p < 0.001$. Error bars are SE.

(C) Novelty-excited neurons' sensitivity to sensory surprise and recency was not significantly correlated with their sensitivity to reward value and information anticipation (from left to right: $\rho = 0.0284$, $p = 0.27$, $\rho = -0.023$, $p = 0.38$, $\rho = 0.030$, $p = 0.25$, $\rho = -0.0036$, $p = 0.89$).

Additional data from reward information viewing procedure are shown in Figure S4.

Ensembles of novelty-responsive neurons had expanded variance in their novelty signals across presentations of distinct novel objects, consistent with the idea that neural systems for novelty detection can have shared response variance, effectively treating some novel objects as “more novel” and others as “less novel”^{45,46} (Figure S5).

Multiple timescales of learning and forgetting

Having delineated important factors underlying novelty processing by neurons in the brain, we next set out to measure their timescales of operation. In everyday life, object novelty is fundamentally linked to a continuous process of learning, as each new novel object gradually becomes familiar with repeated experience. Furthermore, this learning can occur at multiple timescales; sometimes rapidly, sometimes slowly, and sometimes interrupted by forgetting. To investigate the timescales of this novelty-familiarity learning, our behavioral procedure (Figure 1) included Type 4 trials in which sequences of three objects could contain novel objects that sometimes repeated across experimental sessions across multiple days, for up to 5 days (STAR Methods). As a result, these “repeating novel” objects

underwent a novelty-to-familiarity transformation, allowing us to measure each neuron's responses during different stages of learning.

We found that the novelty-excited neuron population's average novelty-related activity reflected a gradual learning process, marked by repeated cycles of rapid within-day learning in each session, followed by substantial between-session forgetting (Figure 6). To quantify this across the population of novelty-excited neurons while controlling for novelty-unrelated sensory adaptation, we normalized neural responses to repeating novel objects based on the responses to fully novel and fully familiar objects in the same trial type and during similar epochs of the behavioral session (STAR Methods).

On Day 1 of exposure to a repeating novel object, the population response rapidly learned to differentiate them from truly novel objects even after a few exposures (Figure 6A). That is, as a novel object repeated within a day, the average novelty-related response of novelty neurons declined. Furthermore, there was also a rapid decline in the learning rate—the fraction of novelty-related activity that disappeared with each exposure to the object. To quantify this, we calculated a measure of the

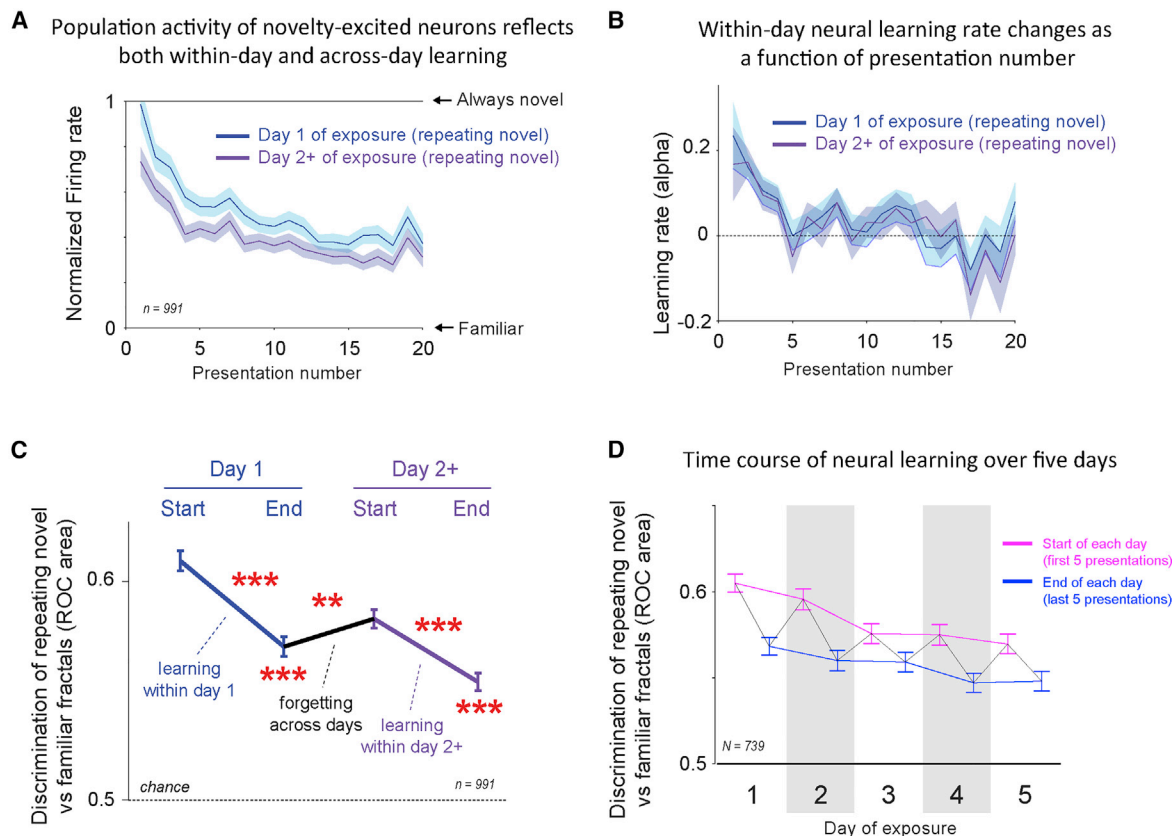


Figure 6. Dynamics of learning and forgetting in novelty-excited neurons

(A) Novelty-excited neuron population response as a function of object exposure. Firing rates are normalized here so that the response is 0 to familiar objects and 1 to always novel objects (STAR Methods). Shaded area is SE.

(B) Novelty-excited neuron population learning rate decreases over the course of each day.

(C) Quantification of within-day and across-day novelty-familiarity transformations. The y axis is the population mean AUC of the ROC for discriminating responses to repeating novel fractals versus familiar fractals. This is quantified for the first 5 (start) and last 5 (end) presentations of each repeating novel object on each day. Error bars are SE. * $p < 0.05$, ** $p < 0.01$, *** $p < 0.001$ (signed-rank tests).

(D) Novelty-excited neurons across-day novelty-familiarity transformations over the course of 5 days (Monkey S; STAR Methods). The y axis is the area under the ROC curve comparing responses to repeating novel fractals versus familiar fractals. Shown are data from the first 5 (magenta) and last 5 (blue) presentations of each fractal in each session. Supplemental analyses of surprise during learning, as well as area by area heterogeneity of learning and forgetting is in Figure S6.

neural learning rate from each individual object exposure. This analysis revealed that at the population level the neural learning rate started high and then rapidly declined over the course of the day (Figure 6B). Importantly, this was found despite controlling for any potentially confounding impact of arousal or task engagement on the time course of the novelty-familiarity transformation (STAR Methods).

Despite their rapid within-session learning, these neurons did not retain their learning perfectly across sessions. Instead, they showed clear evidence of substantial between-session forgetting (Figure 6C). When the same neurons were presented with repeating novel fractals that had been experienced for 2+ days, their initial response was substantially lower than their response to a completely new fractal, indicating some retention of learning (Day 2+ start < Day 1 start, $p < 0.0001$, paired signed-rank test). However, it was also substantially higher than their response to a repeating novel fractal at the end of the first day, indicating substantial forgetting or loss of access to the prior learning (Day 2+ start > Day 1 end, $p = 0.0099$, paired signed-

rank test). Note that this is distinct from the pattern one would expect if neural memories of objects are enhanced following overnight rest between training sessions.⁴⁷ If that was the case, rest should cause neurons to treat the repeating novel object more similarly to a fully familiar object (“overnight or between-session learning”); instead, neurons treated it more similarly to a fully novel object (“overnight or between-session forgetting”). This resembles the “spontaneous recovery” observed in multiple forms of sensory, motor, and motivational learning,^{48–51} and could occur due to the passage of time, rest, or other factors. Thus, on Day 2+, this neural population had to re-start its learning process from an earlier point on the learning curve.

The time course of novelty learning in the novelty-responsive population followed a saw tooth pattern, marked by cycles of within-day learning followed by partial across-day forgetting (Figure 6C). This pattern continued on each day for up to the full 5 days of exposure tested in this experiment, as the population response to the repeating novel fractals gradually

progressed toward familiarity (Figure 6D). The population average response to repeating novel fractals never became fully identical to familiar fractals (Figure 6C, $p < 0.0001$; Figure 5D, $p < 0.0001$, signed-rank test relative to 0.5), which is expected since the familiar fractals had been previously viewed many times (1,000+ exposures). Interestingly, the population made quite similar learning progress each day; the learning rate had a remarkably similar magnitude and time course over the session for fractals regardless of their number of days of exposure (Figure 6B, Day 1 versus Day 2).

Some of the novel objects we encounter in life are only relevant to our immediate situation, but others have long-term importance and must be committed to long-term memory.⁵² Therefore, it would be ideal if the brain contained neural networks with different learning rates to handle this diversity. It has been proposed that the brain contains reservoirs of neurons with different timescales of motor learning, including “fast” neural systems that both learn and forget quickly, and “slow” systems that both learn and forget slowly.^{48,49} This could be also the case for novelty learning. Alternately, it is possible that novelty-responsive neurons throughout the brain learn and forget in lock step with each other, cooperating to form a single, unified representation of each object’s degree of novelty. This would be analogous to theories of motivated behavior, which propose that key motivational variables, such as the values of states and actions, are computed once and then used by multiple brain areas to guide multiple processes such as learning and decision making.^{53–55}

We tested among these hypotheses and found that novelty-responsive neurons learned in diverse manners. For example, in Figure 7A, the left panel shows an example novelty-responsive neuron recorded in area AVMTc, suggestive of “slow learning, slow forgetting.” That is, this neuron was strongly excited by its first exposure to repeating novel objects (Day 1 start), gradually reduced its response over the course of the day (Day 1 end), had a similar response at the start of further days suggestive of little or no forgetting (Day 2+ start), and produced a learning curve that was similar to the first day but with a pronounced downward shift, suggestive of progressive learning across days (Day 2+ start to end). By contrast, in Figure 7A the right panel shows a second AVMTc novelty-responsive neuron with very different learning curves, suggestive of “fast learning, fast forgetting.” This neuron learned at a considerably faster rate on Day 1: by the end of the day its response to repeating novel objects was very close to fully familiar objects. However, this neuron also had considerably greater forgetting: it almost completely “reset” its novelty response on Day 2+, so that the learning curve on Day 2+ had only a little downward shift from Day 1. Thus, while this neuron learned rapidly within each day, it was unable to retain and compound this learning fully across days.

To quantify the time course of novelty-familiarity transformations in single neurons, we calculated statistically independent indexes of how much a neuron learned within a day and forgot across days (Figure 6C; STAR Methods) and assessed the relationship between learning and forgetting. The two indices were strongly correlated (Figure 7C, $\rho = 0.371$, $p < 0.0001$, Spearman’s rank correlation). This correlation was driven by true variation across neurons in their learning-related activity, not by

variations across session in the animal’s learning process, because it remained similarly strong after subtracting out session-level effects (Figure S6B). These results indicate that neurons that learned more within Day 1 also tended to forget more across days. Moreover, while within brain regions these types of neurons were intermingled (e.g., the cells in Figure 7A), we did observe an anatomical trend that strongly corroborates the results of Figure 6C: brain areas that on average had greater within-day learning also had greater across-day forgetting (Figure 7C). Most areas had positive learning and forgetting indexes, while hippocampus and anterior entorhinal cortex had trends for negative forgetting indexes, perhaps consistent with consolidation strengthening memories across days (Figure S6C). This result supports theories that anatomical or circuit differences can support learning on different timescales^{56–61} and provides evidence that this is the case specifically in the realm of novelty-to-familiarity transformations.

DISCUSSION

Current theories put forward distinct models in which novelty is either derived from recency judgments or conceptualized as a form of sensory surprise. Here, we assessed these mechanisms with high-channel electrophysiology and determined that object novelty arises with both computations of recency and surprise, suggesting that novelty detection and memory-related functions are supported by diverse mechanisms, including those linked to predictive coding.

Previous work identified distinct neuronal groups in AVMTc that signaled novelty and recency.⁸ However, that work did not assess the relationships between novelty and recency or novelty and surprise. Also, studies in humans examined how novelty and recency, or novelty and surprise, modulate bulk average brain activity.^{35,62–67} However, they did not establish whether these variables are represented by the same or different groups of neurons or voxels. Our data replicate the findings that AVMTc is a key node of novelty processing and provide a first demonstration for the linkage between recency, surprise, and novelty computations suggested by theory.^{9,68,69} Notably, we could have found instead that novelty sensitivity was not correlated or negatively correlated to recency or surprise. In some sense, within a single pool of neurons such as AVMTc, this could have been a more efficient mode of information encoding.⁷⁰ The deviation from efficiency could further suggest that the relationships between novelty and sensory surprise and recency are important for novelty detection.

Our data do not indicate that novelty, recency, and sensory surprise are always treated identically by the brain.^{9,71} In fact, we found several differences in their relationship across areas (Figure 4). For example, in AVMTc many novelty-sensitive neurons were sensitive to sensory surprise but relatively few were sensitive to recency. By contrast, in basal forebrain and amygdala, novelty-sensitive neurons were commonly sensitive to sensory surprise, recency, or both, consistent with the wide-ranging roles of these regions in memory, sensory processing, and associative learning.^{37,72–79} However, in spite of these differences, across all recorded brain areas and within a large number of individual areas, there was a positive correlation between coding of novelty, recency, and sensory

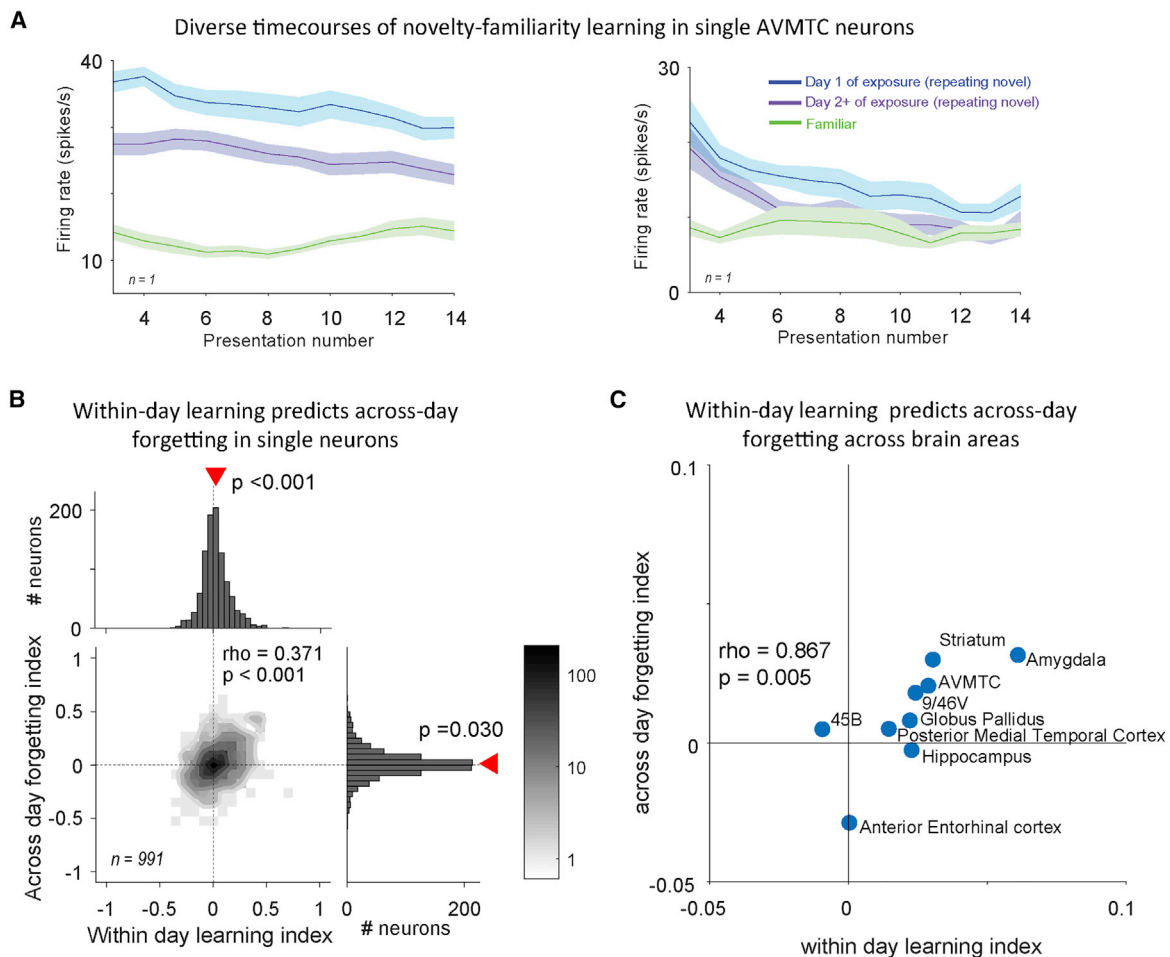


Figure 7. Multiple rates of learning and forgetting across neurons and across brain areas

(A) Left: activity of an example AVMTC neuron with slow, progressive learning over the course of multiple sessions. This plot was made by quantifying activity using a sliding window of 5 object presentations, advanced in steps of 1 object presentation; shaded area is SE. Right: a second example AVMTC neuron that learned rapidly within each day but almost completely reset its learning curve across days.

(B) Correlation between indexes of neural learning within day (x axis) and forgetting across days (y axis). The heatmap shows the joint distribution of the two indexes, and the histograms show the marginal distributions of each index. A positive within-day learning index indicates responses to repeating novel fractals become relatively more like responses to familiar fractals at Day 1 end than Day 1 start. A positive across-day forgetting index is an analogous comparison between Day 1 end and Day 2 start (also see Figure S6).

(C) Heterogeneity in average learning and forgetting indices across brain areas. Scatterplot showing the distribution of the mean within-day learning index and mean across-day forgetting index of each brain area.

surprise. We interpret the results to mean that neurons sensitive to these variables can be functionally linked in support of novelty detection.

In fact, novelty and surprise can arise due to many sources. Sensory surprise indices (Figure 1) measure surprise due to probability of seeing an object. However, other forms of surprises, such as during sequence violations (Figures S3B–S3D), also incorporate surprise due to violations in beliefs about the structure of the world. Novelty can be expected or unexpected (Zhang et al.,³ Barto et al.,¹⁸ and Monosov;³⁷ in our data sensitivities to unexpected novelty in Type 4 trials and to expected novelty in Type 1 trials were highly correlated, $\rho = 0.3582$; $p < 0.001$). While expected and unexpected novelty or surprises formally could have different roles in learning,⁸⁰ in naturalistic contexts, the line between expectedness and unexpectedness

is never clear—agents need to monitor all surprising and novel events to detect changes in contexts and distributions of outcomes and events.³⁷ This notion is supported by the linkage we see between novelty sensitivity and different forms of sensory surprise across many brain areas (Figures 3, 4, and S3).

That said, we also found important differences between distinct forms of surprise among the brain areas. For example, in the basal forebrain coding of novelty was negatively correlated with coding of expected sensory surprises, but positively correlated with coding of unexpected violations of the sequential structure of the task.³ The striatum and the hippocampus also seemed to have many neurons that were sensitive to violations of sequence structure. By contrast, the AVMTC and the amygdala had relatively more neurons that were sensitive to expected sensory surprises.

Neuronal novelty-familiarity transformations occurred with multiple, heterogeneous time courses, with some neurons learning slowly but steadily over the course of multiple days, and others learning rapidly within each day but retaining little across days. This may support adaptive behavior in a world in which some objects are only relevant for short periods of time, while others must be remembered for a lifetime. This is akin to theories of sensorimotor learning and adaptation in which the motor system must adjust to perturbations during movements that are unlikely to ever again challenge the system, and also to slow permanent changes, like age-related changes in the body or permanent changes in the task.⁴⁸ It has been suggested that to support such fast and slow changes the brain may have evolved fast and slow learning systems,^{49,59,81} that also forget quickly or slowly, respectively. We found evidence for similar mechanisms for novelty detection. Neurons underwent novelty-to-familiarity transformations at a spectrum of timescales, with some learning rapidly and others learning slowly. These timescales of learning were reflected in a consistent manner across time; neurons which learned rapidly within a session also tended to have greater spontaneous recovery across sessions.

We observed that neurons in AVMTC with strong selective activations by novel objects also had high sensory surprise indices, reflecting strong differential activation by objects that were predicted to appear with a low probability (trial Type 3) versus high probability (trial Type 2). Kaliukhovich and Vogels⁸² found that inferotemporal (IT) neurons, lateral to AVMTC (Figure S7), responded more strongly to an object in blocks when it had a 10% probability of appearing rather than a 90% probability of appearing, and this adapted rapidly to recent stimulus history. These responses were insensitive to the prior probability distribution of alternative objects that could have been presented, to either a narrow distribution (a single alternative object with a 90% probability of appearing) or to a wide one (9 different alternative objects which each had a 10% probability of appearing). Meyer and Olson⁸³ trained monkeys with stable sequences of objects (i.e., object A → B, A → B, C → D, C → D) and after extensive training violated the monkeys' expectations (i.e., C → B). IT activations were higher in response to these sequence violation events, which they attributed to the suppression of predicted stimuli.^{83,84} Bell et al.⁸⁵ reported that IT responses to faces were suppressed during periods when faces were presented with high probability.^{26,85} These papers suggest that surprise effects in IT could be due to computations tightly linked to object presentation probability. Our own data in neighboring brain areas, including AVMTC, are consistent with this interpretation.

It is highly possible that sensory surprise signals in different brain regions regulate different predictions and behavioral control algorithms. Such diversity can theoretically support the distinct strategies of novelty detection that have been developed in machine learning.³⁰ For example, different brain areas or circuits may implement novelty detection based on comparing sensory input with explicit sensory memories,^{86,87} such as in Hopfield networks,^{9,20,68} or with beliefs about the probability of particular objects and the variability of objects in the environment. A diversity of novelty detection and memory encoding mechanisms may be supported by the heterogeneous

timescales of learning and forgetting that we observed within individual brain regions, and across the brain, but how remains to be studied in biological and artificial neural networks.

STAR★METHODS

Detailed methods are provided in the online version of this paper and include the following:

- **KEY RESOURCES TABLE**
- **RESOURCE AVAILABILITY**
 - Lead contact
 - Materials availability
 - Data and code availability
- **EXPERIMENTAL MODEL AND SUBJECT DETAILS**
- **METHOD DETAILS**
 - Object viewing procedure
 - Usage of fractals as visual stimuli
 - Reward information viewing procedure
- **QUANTIFICATION AND STATISTICAL ANALYSIS**
 - Normalization of firing rate in the learning analysis
 - Learning rate analysis
 - Within day learning index
 - Across day forgetting index
 - Control for Figure 7B
 - Pupil analysis
 - Correlation analyses
 - Classifier analyses
 - Cross-validation
 - Noise correlation analysis
 - Noise variance analysis
 - Stability of object selectivity across sessions
 - Hierarchical clustering of brain areas

SUPPLEMENTAL INFORMATION

Supplemental information can be found online at <https://doi.org/10.1016/j.cub.2022.03.064>.

ACKNOWLEDGMENTS

This work is supported by the National Institute of Mental Health under award numbers R01MH110594 and R01MH116937 to I.E.M., by the Army Research Office 78259-NS-MUR, and by the McKnight Foundation award to I.E.M. The optimization of array technology was originally supported by the Defense Advanced Research Projects Agency (DARPA) Biological Technologies Office (BTO) ElectRx program under the auspices of Dr. Doug Weber through the CMO Grant/Contract no. HR0011-16-2-0022. We are grateful for helpful comments from Drs. Ali Ghazizadeh, Carl R. Olson, David L. Sheinberg, and Konrad P. Kording.

AUTHOR CONTRIBUTIONS

K.K., I.E.M., and K.Z. performed the neuronal recordings, and K.Z., E.S.B.-M., and I.E.M. analyzed the neural data. K.Z. performed spike sorting. F.S. performed array localization and analyses. I.E.M. guided the research and wrote the manuscript with K.Z. and E.S.B.-M.

DECLARATION OF INTERESTS

The authors declare no competing interests.

Received: January 10, 2022

Revised: February 28, 2022

Accepted: March 24, 2022

Published: April 18, 2022

REFERENCES

- Jaegle, A., Mehrpour, V., and Rust, N. (2019). Visual novelty, curiosity, and intrinsic reward in machine learning and the brain. *Curr. Opin. Neurobiol.* *58*, 167–174.
- Gottlieb, J., Oudeyer, P.-Y., Lopes, M., and Baranes, A. (2013). Information-seeking, curiosity, and attention: computational and neural mechanisms. *Trends Cogn. Sci.* *17*, 585–593.
- Zhang, K., Chen, C.D., and Monosov, I.E. (2019). Novelty, salience, and surprise timing are signaled by neurons in the basal forebrain. *Curr. Biol.* *29*, 134–142.e3.
- Tiitinen, H., May, P., Reinikainen, K., and Näätänen, R. (1994). Attentive novelty detection in humans is governed by pre-attentive sensory memory. *Nature* *372*, 90–92.
- Tapper, A.R., and Molas, S. (2020). Midbrain circuits of novelty processing. *Neurobiol. Learn. Mem.* *176*, 107323.
- Anderson, B., Mruzek, R.E.B., Kawasaki, K., and Sheinberg, D. (2008). Effects of familiarity on neural activity in monkey inferior temporal lobe. *Cereb. Cortex* *18*, 2540–2552.
- Joshua, M., Adler, A., and Bergman, H. (2010). Novelty encoding by the output neurons of the basal ganglia. *Front. Syst. Neurosci.* *3*, 20.
- Xiang, J.-Z., and Brown, M.W. (1998). Differential neuronal encoding of novelty, familiarity and recency in regions of the anterior temporal lobe. *Neuropharmacology* *37*, 657–676.
- Bogacz, R., Brown, M.W., and Giraud-Carrier, C. (2001). Model of cooperation between recency, familiarity and novelty neurons in the perirhinal cortex. *Neurocomputing* *38*, 1121–1126.
- Ghazizadeh, A., Griggs, W., and Hikosaka, O. (2016). Ecological origins of object salience: reward, uncertainty, aversiveness, and novelty. *Front. Neurosci.* *10*, 378.
- Petrides, M., Alvisatos, B., and Frey, S. (2002). Differential activation of the human orbital, mid-ventrolateral, and mid-dorsolateral prefrontal cortex during the processing of visual stimuli. *Proc. Natl. Acad. Sci. USA* *99*, 5649–5654.
- Ranganath, C., and Rainer, G. (2003). Neural mechanisms for detecting and remembering novel events. *Nat. Rev. Neurosci.* *4*, 193–202.
- Kumaran, D., and Maguire, E.A. (2007). Which computational mechanisms operate in the hippocampus during novelty detection? *Hippocampus* *17*, 735–748.
- Ogasawara, T., Sogukpinar, F., Zhang, K., Feng, Y.-Y., Pai, J., Jezzini, A., and Monosov, I.E. (2022). A primate temporal cortex–zona incerta pathway for novelty seeking. *Nat. Neurosci.* *25*, 50–60.
- Berlyne, D.E. (1970). Novelty, complexity, and hedonic value. *Percept. Psychophys.* *8*, 279–286.
- Berlyne, D.E. (1950). Novelty and curiosity as determinants of exploratory behaviour. *Br. J. Psychol.* *41*, 68.
- Berlyne, D.E. (1957). Uncertainty and conflict: a point of contact between information-theory and behavior-theory concepts. *Psychol. Rev.* *64*, 329–339.
- Barto, A., Mirolli, M., and Baldassarre, G. (2013). Novelty or surprise? *Front. Psychol.* *4*, 907.
- Berlyne, D.E. (1960). *Conflict, Arousal, and Curiosity* (McGraw-Hill Book Company).
- Bogacz, R., Brown, M.W., and Giraud-Carrier, C. (2001). Model of familiarity discrimination in the perirhinal cortex. *J. Comput. Neurosci.* *10*, 5–23.
- Egner, T., Monti, J.M., and Summerfield, C. (2010). Expectation and surprise determine neural population responses in the ventral visual stream. *J. Neurosci.* *30*, 16601–16608.
- Homann, J., Koay, S.A., Glidden, A.M., Tank, D.W., and Berry, M.J. (2017). Predictive coding of novel versus familiar stimuli in the primary visual cortex. Preprint at bioRxiv. <https://doi.org/10.1101/197608>.
- Kumaran, D., and Maguire, E.A. (2007). Match mismatch processes underlie human hippocampal responses to associative novelty. *J. Neurosci.* *27*, 8517–8524.
- Reichardt, R., Polner, B., and Simor, P. (2020). Novelty manipulations, memory performance, and predictive coding: the role of unexpectedness. *Front. Hum. Neurosci.* *14*, 152.
- Schwartenbeck, P., FitzGerald, T., Dolan, R.J., and Friston, K. (2013). Exploration, novelty, surprise, and free energy minimization. *Front. Psychol.* *4*, 710.
- Vogels, R. (2016). Sources of adaptation of inferior temporal cortical responses. *Cortex* *80*, 185–195.
- Fahy, F.L., Riches, I.P., and Brown, M.W. (1993). Neuronal activity related to visual recognition memory: long-term memory and the encoding of recency and familiarity information in the primate anterior and medial inferior temporal and rhinal cortex. *Exp. Brain Res.* *96*, 457–472.
- Li, L., Miller, E.K., and Desimone, R. (1993). The representation of stimulus familiarity in anterior inferior temporal cortex. *J. Neurophysiol.* *69*, 1918–1929.
- Hart, E.W., and Jacoby, J. (1973). Novelty, recency, and scarcity as predictors of perceived newness. In *Proceedings of the Annual Convention of the American Psychological Association* (American Psychological Association).
- Miljković, D. (2010). Review of novelty detection methods. In *The 33rd International Convention MIPRO* (IEEE Publications), pp. 593–598.
- Miyashita, Y., Higuchi, S., Sakai, K., and Masui, N. (1991). Generation of fractal patterns for probing the visual memory. *Neurosci. Res.* *12*, 307–311.
- Yamamoto, S., Monosov, I.E., Yasuda, M., and Hikosaka, O. (2012). What and where information in the caudate tail guides saccades to visual objects. *J. Neurosci.* *32*, 11005–11016.
- Yasuda, M., Yamamoto, S., and Hikosaka, O. (2012). Robust representation of stable object values in the oculomotor basal ganglia. *J. Neurosci.* *32*, 16917–16932.
- Kafkas, A., and Montaldi, D. (2015). The pupillary response discriminates between subjective and objective familiarity and novelty. *Psychophysiology* *52*, 1305–1316.
- Kafkas, A., and Montaldi, D. (2018). How do memory systems detect and respond to novelty? *Neurosci. Lett.* *680*, 60–68.
- Võ, M.L.H., Jacobs, A.M., Kuchinke, L., Hofmann, M., Conrad, M., Schacht, A., and Hutzler, F. (2008). The coupling of emotion and cognition in the eye: introducing the pupil old/new effect. *Psychophysiology* *45*, 130–140.
- Monosov, I.E. (2020). How outcome uncertainty mediates attention, learning, and decision-making. *Trends Neurosci.* *43*, 795–809.
- Turchi, J., Chang, C., Ye, F.Q., Russ, B.E., David, K.Y., Cortes, C.R., Monosov, I.E., Duyn, J.H., and Leopold, D.A. (2018). The basal forebrain regulates global resting-state fMRI fluctuations. *Neuron* *97*, 940–952.e4.
- White, J.K., Bromberg-Martin, E.S., Heilbronner, S.R., Zhang, K., Pai, J., Haber, S.N., and Monosov, I.E. (2019). A neural network for information seeking. *Nat. Commun.* *10*, 5168.
- Jezzini, A., Bromberg-Martin, E.S., Trambaiolli, L.R., Haber, S.N., and Monosov, I.E. (2021). A prefrontal network integrates preferences for advance information about uncertain rewards and punishments. *Neuron* *109*, 2339–2352.e5.
- Ghazizadeh, A., Fakharian, M.A., Amini, A., Griggs, W., Leopold, D.A., and Hikosaka, O. (2020). Brain networks sensitive to object novelty, value, and their combination. *Cereb. Cortex Commun.* *1*, tgaa034.
- Costa, V.D., and Averbeck, B.B. (2020). Primate orbitofrontal cortex codes information relevant for managing explore–exploit tradeoffs. *J. Neurosci.* *40*, 2553–2561.

43. Costa, V.D., Mitz, A.R., and Averbeck, B.B. (2019). Subcortical substrates of explore-exploit decisions in primates. *Neuron* *103*, 533–545.e5.
44. Kakade, S., and Dayan, P. (2002). Dopamine: generalization and bonuses. *Neural Netw.* *15*, 549–559.
45. Meyer, T., and Rust, N.C. (2018). Single-exposure visual memory judgments are reflected in IT cortex. *eLife* *7*, e32259.
46. Mehrpour, V., Meyer, T., Simoncelli, E.P., and Rust, N.C. (2021). Pinpointing the neural signatures of single-exposure visual recognition memory. *Proc. Acad. Sci. USA* *118*, e2021660118.
47. Stickgold, R. (2005). Sleep-dependent memory consolidation. *Nature* *437*, 1272–1278.
48. Smith, M.A., Ghazizadeh, A., and Shadmehr, R. (2006). Interacting adaptive processes with different timescales underlie short-term motor learning. *PLoS Biol.* *4*, e179.
49. Kording, K.P., Tenenbaum, J.B., and Shadmehr, R. (2007). The dynamics of memory as a consequence of optimal adaptation to a changing body. *Nat. Neurosci.* *10*, 779–786.
50. Rescorla, R.A. (2004). Spontaneous recovery. *Learn. Mem.* *11*, 501–509.
51. Pavlov, I.P. (1960). *Conditioned Reflex: An Investigation of the Physiological Activity of the Cerebral Cortex* (Dover Publications).
52. Hikosaka, O., Yamamoto, S., Yasuda, M., and Kim, H.F. (2013). Why skill matters. *Trends Cogn. Sci.* *17*, 434–441.
53. Schultz, W., Dayan, P., and Montague, P.R. (1997). A neural substrate of prediction and reward. *Science* *275*, 1593–1599.
54. Padoa-Schioppa, C., and Cai, X. (2011). The orbitofrontal cortex and the computation of subjective value: consolidated concepts and new perspectives. *Ann. NY Acad. Sci.* *1239*, 130–137.
55. Schultz, W. (2002). Getting formal with dopamine and reward. *Neuron* *36*, 241–263.
56. Monosov, I.E., Haber, S.N., Leuthardt, E.C., and Jezzini, A. (2020). Anterior cingulate cortex and the control of dynamic behavior in primates. *Curr. Biol.* *30*, R1442–R1454.
57. Spitmaam, M., Seo, H., Lee, D., and Soltani, A. (2020). Multiple timescales of neural dynamics and integration of task-relevant signals across cortex. *Proc. Natl. Acad. Sci. USA* *117*, 22522–22531.
58. Bromberg-Martin, E.S., Matsumoto, M., Nakahara, H., and Hikosaka, O. (2010). Multiple timescales of memory in lateral habenula and dopamine neurons. *Neuron* *67*, 499–510.
59. Kim, H.F., and Hikosaka, O. (2013). Distinct basal ganglia circuits controlling behaviors guided by flexible and stable values. *Neuron* *79*, 1001–1010.
60. Murray, J.D., Bernacchia, A., Freedman, D.J., Romo, R., Wallis, J.D., Cai, X., Padoa-Schioppa, C., Pasternak, T., Seo, H., Lee, D., and Wang, X.-J. (2014). A hierarchy of intrinsic timescales across primate cortex. *Nat. Neurosci.* *17*, 1661–1663.
61. Cavanagh, S.E., Wallis, J.D., Kennerley, S.W., and Hunt, L.T. (2016). Autocorrelation structure at rest predicts value correlates of single neurons during reward-guided choice. *eLife* *5*, e18937.
62. Dudukovic, N.M., and Wagner, A.D. (2007). Goal-dependent modulation of declarative memory: neural correlates of temporal recency decisions and novelty detection. *Neuropsychologia* *45*, 2608–2620.
63. Law, J.R., Flanery, M.A., Wirth, S., Yanike, M., Smith, A.C., Frank, L.M., Suzuki, W.A., Brown, E.N., and Stark, C.E. (2005). Functional magnetic resonance imaging activity during the gradual acquisition and expression of paired-associate memory. *J. Neurosci.* *25*, 5720–5729.
64. Wessel, J.R., Danielmeier, C., Morton, J.B., and Ullsperger, M. (2012). Surprise and error: common neuronal architecture for the processing of errors and novelty. *J. Neurosci.* *32*, 7528–7537.
65. Strange, B.A., Duggins, A., Penny, W., Dolan, R.J., and Friston, K.J. (2005). Information theory, novelty and hippocampal responses: unpredicted or unpredictable? *Neural Netw* *18*, 225–230.
66. Utzerath, C., Schmits, I.C., Buitelaar, J., and de Lange, F.P. (2018). Adolescents with autism show typical fMRI repetition suppression, but atypical surprise response. *Cortex* *109*, 25–34.
67. Schomaker, J., and Meeter, M. (2015). Short- and long-lasting consequences of novelty, deviance and surprise on brain and cognition. *Neurosci. Biobehav. Rev.* *55*, 268–279.
68. Bogacz, R., and Brown, M.W. (2003). An anti-Hebbian model of familiarity discrimination in the perirhinal cortex. *Neurocomputing* *52*, 1–6.
69. Bogacz, R., and Brown, M.W. (2003). Comparison of computational models of familiarity discrimination in the perirhinal cortex. *Hippocampus* *13*, 494–524.
70. Koay, S.A., Charles, A.S., Thiberge, S.Y., Brody, C., and Tank, D.W. (2021). Sequential and efficient neural-population coding of complex task information. *Neuron* *110*, 328–349.e11.
71. Charles, D.P., Gaffan, D., and Buckley, M.J. (2004). Impaired recency judgments and intact novelty judgments after fornix transection in monkeys. *J. Neurosci.* *24*, 2037–2044.
72. Dal Monte, O., Costa, V.D., Noble, P.L., Murray, E.A., and Averbeck, B.B. (2015). Amygdala lesions in rhesus macaques decrease attention to threat. *Nat. Commun.* *6*, 1–10.
73. Costa, V.D., Dal Monte, O., Lucas, D.R., Murray, E.A., and Averbeck, B.B. (2016). Amygdala and ventral striatum make distinct contributions to reinforcement learning. *Neuron* *92*, 505–517.
74. Peck, C.J., and Salzman, C.D. (2014). The amygdala and basal forebrain as a pathway for motivationally guided attention. *J. Neurosci.* *34*, 13757–13767.
75. Murray, E.A., and Mishkin, M. (1998). Object recognition and location memory in monkeys with excitotoxic lesions of the amygdala and hippocampus. *J. Neurosci.* *18*, 6568–6582.
76. Baxter, M.G., and Murray, E.A. (2002). The amygdala and reward. *Nat. Rev. Neurosci.* *3*, 563–573.
77. Murray, E.A., and Izquierdo, A. (2007). Orbitofrontal cortex and amygdala contributions to affect and action in primates. *Ann. NY Acad. Sci.* *1121*, 273–296.
78. Peck, C.J., Lau, B., and Salzman, C.D. (2013). The primate amygdala combines information about space and value. *Nat. Neurosci.* *16*, 340–348.
79. Everitt, B.J., and Robbins, T.W. (1997). Central cholinergic systems and cognition. *Annu. Rev. Psychol.* *48*, 649–684.
80. Soltani, A., and Izquierdo, A. (2019). Adaptive learning under expected and unexpected uncertainty. *Nat. Rev. Neurosci.* *20*, 635–644.
81. Logothetis, N.K., and Sheinberg, D.L. (1996). Visual object recognition. *Annu. Rev. Neurosci.* *19*, 577–621.
82. Kaliukhovich, D.A., and Vogels, R. (2014). Neurons in macaque inferior temporal cortex show no surprise response to deviants in visual oddball sequences. *J. Neurosci.* *34*, 12801–12815.
83. Meyer, T., and Olson, C.R. (2011). Statistical learning of visual transitions in monkey inferotemporal cortex. *Proc. Natl. Acad. Sci. USA* *108*, 19401–19406.
84. Ramachandran, S., Meyer, T., and Olson, C.R. (2016). Prediction suppression in monkey inferotemporal cortex depends on the conditional probability between images. *J. Neurophysiol.* *115*, 355–362.
85. Bell, A.H., Summerfield, C., Morin, E.L., Malecek, N.J., and Ungerleider, L.G. (2017). Reply to Vinken and Vogels. *Curr. Biol.* *27*, R1212–R1213.
86. Tyulmankov, D., Yang, G.R., and Abbott, L.F. (2022). Meta-learning synaptic plasticity and memory addressing for continual familiarity detection. *Neuron* *110*, 544–557.e8.
87. Dasgupta, S., Sheehan, T.C., Stevens, C.F., and Navlakha, S. (2018). A neural data structure for novelty detection. *Proc. Natl. Acad. Sci. USA* *115*, 13093–13098.
88. Daye, P.M., Monosov, I.E., Hikosaka, O., Leopold, D.A., and Optican, L.M. (2013). pyElectrode: an open-source tool using structural MRI for electrode positioning and neuron mapping. *J. Neurosci. Methods* *213*, 123–131.

89. Ledbetter, N.M., Chen, C.D., and Monosov, I.E. (2016). Multiple mechanisms for processing reward uncertainty in the primate basal forebrain. *J. Neurosci.* *36*, 7852–7864.
90. Dotson, N.M., Hoffman, S.J., Goodell, B., and Gray, C.M. (2017). A large-scale semi-chronic microdrive recording system for non-human primates. *Neuron* *96*, 769–782.e2.
91. Dotson, N.M., Hoffman, S.J., Goodell, B., and Gray, C.M. (2018). Feature-based visual short-term memory is widely distributed and hierarchically organized. *Neuron* *99*, 215–226.e4.
92. Ghazizadeh, A., Griggs, W., and Hikosaka, O. (2016). Object-finding skill created by repeated reward experience. *J. Vis.* *16*, 17.

STAR★METHODS

KEY RESOURCES TABLE

REAGENT or RESOURCE	SOURCE	IDENTIFIER
Deposited data		
Data and figure generation code	This paper	https://github.com/kalfton/Noveltypaper
Experimental models: Organisms/strains		
Rhesus Macaques	PrimGen	Macaca mulatta
	NIH Animal Center at Poolesville	N/A
Software and algorithms		
MATLAB	Mathworks	https://www.mathworks.com/

RESOURCE AVAILABILITY

Lead contact

Further information and requests for resources, data and code should be directed to Dr. Ilya E. Monosov (ilya.monosov@gmail.com).

Materials availability

This study did not generate unique reagents.

Data and code availability

Data and figure generation code is available at <https://github.com/kalfton/Noveltypaper>.

EXPERIMENTAL MODEL AND SUBJECT DETAILS

Two adult male monkeys (*Macaca mulatta*; Monkey L and Monkey S; ages: 7-10 years old) were used for neurophysiological recording experiments. All procedures conform to the Guide for the Care and Use of Laboratory Animals and were approved by the Institutional Animal Care and Use Committee at Washington University.

METHOD DETAILS

Two adult male rhesus monkeys (S and L; *Macaca mulatta*) were used for the electrophysiology experiments. All procedures conformed to the Guide for the Care and Use of Laboratory Animals and were approved by the Washington University Institutional Animal Care and Use Committee. A plastic head holder and plastic recording chamber were fixed to the skull under general anesthesia and sterile surgical conditions. For each monkey, we implanted a semi-chronic high channel count recording drive (LS124; Gray Matter). To aim these micro drives, we first acquired 3T magnetic resonance images of the monkeys' brain. We used these MRIs to aim the two micro drives towards the regions of interest, including the prefrontal cortex and the temporal cortex. We then attached MRI compatible chambers to the skull using MRI compatible ceramic screws (Thomas). After the animals recovered, we performed MRI with fiducials such that we could estimate and reconstruct the path of each electrode.^{39,88–91} Next, we implanted both animals with 124-channel micro drives. These are detailed here: <https://www.graymatter-research.com/documentation-manuals>. Following craniotomy, we sealed the chamber and used a port to assess whether bacterial growth occurred. Following this safety precaution, we implanted the recording drives containing the electrodes and lowered all channels immediately beyond the dura. In this way, we minimized the impact of post-op dura thickening on the electrode impedance and trajectory. Data from electrode-channels were included in the study if (1) post-op CT images showed that the electrodes were in the brain and were following a trajectory that could be reconstructed, (2) if the electrode-channel produced single units during the history of the array neuronal recordings, and (3) if the post-op impedance was $>0.2\text{M}\Omega$ or single units were observed. This approach produced 108/124 channels in Monkey L and 124/124 channels in Monkey S. A key difference in success was due to the use of glass coated electrodes (Alpha Omega) in Monkey S versus thinner epoxy electrodes in Monkey L (FHC). The semi chronic drive contained electrodes with 1.5mm spacing. Signal acquisition (including amplification and filtering) was performed using Plexon 40kHz recording system. Action potentials were identified using a template matching based algorithm (Kilosort2) to sort the data, and then we minimized cluster over-splitting, removed artifacts, and selected isolated clusters. All recording and reconstruction procedures are as in Ogasawara et al.¹⁴ (Figure S7).

Object viewing procedure

This behavioral procedure was designed to investigate how novelty and novelty-related events are encoded. In each trial of the task, a fixation point appeared at the center of the screen (~ 0.5 degrees). The shape of the fixation point indicated the trial type (i.e. each of the four trial types had a distinct fixation point shape). The animal was required to fixate on the fixation point for 400ms to initiate the trial. After that, the monkeys were shown a sequence of three fractals at the center of the screen, during which time the fixation point remained at the center of the screen and animals were required to maintain fixation. Each fractal was shown for 250ms and there was a 250ms inter-fractal-interval between fractal presentations. If the animal broke fixation at any time before the third fractal disappeared, or did not start to fixate on the fixation point within 5s after the point appeared, this was counted as an error, the trial stopped immediately, a sound indicating an error was played, and the same trial started again after the inter trial interval (ITI, ~ 5 s). If the animal successfully fixated till the end of the 3rd fractal, the screen went blank for a randomized time (200ms-1000ms), then a reward dot, visually distinct from the fixation point dot at the start of the trial, appeared in one of four peripheral positions (~ 10 degrees above/below/left/right of the center of the screen). The monkeys needed to saccade to this dot for reward (Figure 1B); if the monkey failed to do so within 5s, the reward dot disappeared, a sound indicating an error was played, and the same trial started again after the ITI.

There were four trial types (Type 1 through Type 4), which respectively occurred with 12.5%, 25%, 25%, and 37.5% probability. Each trial type contained a distinct set of fractals. In type 1 trials, the 2nd fractal was always a novel fractal which was generated at the start of the trial, while the other two fractals were fixed familiar fractals (i.e. the same two familiar fractals were always used for Trial Type 1). In Type 2 trials, all three fractals were familiar fractals presented in a fixed order. There were 2 possible distinct sets of three familiar fractals. On each trial, one of these two sets was randomly picked to be shown, and each set was always shown in the same fixed sequence (i.e. always $A \rightarrow B \rightarrow C$ or $D \rightarrow E \rightarrow F$; except for rare 'sequence violation' trials, explained below). We used Type 1 and Type 2 trials to test whether a neuron responds to the predictable onset of a novel stimulus (2nd fractal on Trial Type 1) vs. predictable onset of a familiar stimulus (2nd fractal on Trial Type 2). In trial type 3, just like trial type 2, there were also two distinct sets of three familiar fractals, and one of these two sets was randomly picked to be shown on each trial. However, unlike trial type 2, each presented fractal was drawn randomly with replacement from the picked set. Thus, on each trial, the three presented fractals were drawn from the same set, but they could occur in a randomized order (e.g. $A \rightarrow B \rightarrow C$, $B \rightarrow A \rightarrow C$, etc.) and could include repeats of the same fractal while omitting other fractals (e.g. $A \rightarrow B \rightarrow A$, $B \rightarrow B \rightarrow B$, etc.). This trial type was designed to study surprise and recency, because unlike trial type 2 each individual fractal could not be fully predicted, and there were variable time durations between each time the animal was exposed to a given fractal. In addition, to create sequence violation events, in trial type 2, with 5% probability in each of the 2nd or 3rd positions in the sequence, the familiar fractal that would have been presented on that trial was replaced with the familiar fractal in the corresponding position of the other set (e.g. $A \rightarrow E \rightarrow C$ or $A \rightarrow B \rightarrow F$). Thus during a sequence violation, the violating fractal had an unexpected identity, but all fractals still had their normal positions in the sequence and normal proximity to reward.

In trial type 4, there were 3 types of fractals: always novel fractals, repeating novel fractals and familiar fractals. We used this trial type to study neurons' novelty-familiarity transformation. The always novel fractals were generated before each trial. The familiar fractals were 4 fractals which were always the same and were exposed to the monkey thousands of times. The repeating novel fractals were slightly different for each animal. In Monkey S's version, 4 repeating novel fractals were generated before the task each day. On the next working day, 2 of those 4 fractals were deleted, while the other 2 were saved up to 5 working days and then deleted. Thus, there were always 12 repeating novel fractals in each session: 4 fractals that were on their 1st day of exposure, 2 that were on their 2nd day, 2 that were on their 3rd day, and so on (Figure 1B). On each trial, each fractal in each position of the sequence was picked randomly and independently from these types. Thus, the probability of presenting each fractal was: 1/17 for each of the 12 possible repeating novel fractals; 1/17 for each of the 4 possible familiar fractals; and 1/17 to show an always novel fractal. In Monkey L's version, 4 repeating novel fractals were generated before the task each day and were deleted on the next working day, and another 2 repeating novel fractals were generated on the first day of recording and were replaced after 5 days. Thus, there were always 6 repeating novel fractals in each session: 4 fractals that were on their 1st day, and 2 fractals that could be on either their 1st, 2nd, 3rd, 4th, or 5th day. On each trial, each fractal in each position of the sequence was picked randomly and independently from these types. Thus, the probability of presenting each fractal was: 1/11 for each repeating novel fractal, 1/11 for each familiar fractal, and 1/11 to show an always novel fractal.

Usage of fractals as visual stimuli

All visual fractals were generated using the same previously described algorithm.^{3,14,31–33} In previous work, monkeys strongly and rapidly discriminated novel fractals from the familiar fractals^{10,41,52} and learned to distinguish between hundreds of fractals (e.g. associating different individual fractals with reward or no reward).^{33,52,92} After this training, they still readily detected that a new fractal is novel and not part of a well-learned set.^{10,52} Using an algorithmic procedure for generating stimuli has key advantages over the alternative of drawing from a library of objects (e.g. photographs of objects or scenes), including being able to generate a very large number of novel objects on-demand on a trial by trial basis, and ensuring that all stimuli have similar gross visual properties (e.g. size, degree of radial symmetry, etc.) to minimize the possibility that response differences between conditions could be caused by the stimulus sets containing visual features that just happen to vary with the task variables.

Reward information viewing procedure

This behavioral procedure was a variant of the information viewing task we previously used to investigate how reward and information about reward are encoded in the brain (White et al.³⁹). On each trial of the task, a fixation point appeared at the center of the screen

which the monkey was required to fixate for 300ms to initiate the trial. After the trial was successfully initiated, the fixation point disappeared, and a fractal Cue1 appeared on the screen for 1s. This cue indicated the probability of large reward delivery. Then a fractal Cue2 appeared at the center of Cue1. On informative trials, Cue2 provided information about whether a big reward was going to be delivered. Both cues stayed on the screen for another 1s. Monkeys were required to fixate as long as Cue1 or Cue2 were on the screen. If the monkey broke fixation or did not fixate to start the trial 5s after the fixation point appeared, this was counted as an error, the trial stopped immediately, a sound indicating an error was played, and the same trial started again after the ITI (2s). After the cues disappeared the reward was delivered, which was always either a large or small amount of juice. Two blocks of trials alternated: In the informative block, Cue2 informed the monkey whether the big reward was going to be delivered, while in the non-informative block Cue2 was randomized and hence provided no new information about the outcome. In both blocks, Cue1 indicated the probability of big juice delivery (0%, 50%, or 100%). In each block, there were two possible Cue1 stimuli for each probability (one of which was randomly chosen to present on each trial), thus there were a total of 12 unique Cue1 fractals). In the informative block, there were 4 possible Cue2 stimuli, 2 indicating big reward and 2 indicating small reward. On each trial, one of the 2 stimuli corresponding to the trial's upcoming reward outcome was randomly chosen to be presented. In the non-informative block, there were 4 distinct possible Cue2 stimuli. On each trial, one of these 4 stimuli was randomly chosen to be presented (and hence conveyed no information about the reward outcome).

QUANTIFICATION AND STATISTICAL ANALYSIS

For all analyses in the object viewing procedure, unless otherwise stated, each neuron's responses to visual fractal objects were measured as the mean firing rate in the 500ms time window starting from fractal onset. When permutations were used to assess significance or obtain confidence intervals, we permuted 10000 times.

The novelty index was quantified by AUC of ROC (area under the curve of the receiver operating characteristic curve) comparing the neural responses to the novel fractals in the second position of Type 1 trials versus the familiar fractals in the second position in Type 2 trials. We then subtracted 0.5 from the AUC such that numbers higher than 0 indicated that the neuron had a higher firing rate to the novel fractals than familiar fractals, and multiplied the result by 2 such that the range of the index was [-1, 1]. The significance of this index was tested by a rank sum test (threshold: $p < 0.01$).

A novelty responsive neuron was defined as a neuron with a significant novelty index. A novelty-excited neuron was a novelty responsive neuron with its novelty index larger than 0, while a novelty-inhibited neuron was a novelty responsive neuron with its novelty index less than 0. We used analogous definitions for recency responsive neurons, sensory surprise responsive neurons, recency-excited neurons, etc.

The sensory surprise index was quantified by AUC of ROC of each neuron's responses to the familiar fractals in the third place in Type 3 trials versus the familiar fractals in the third place in Type 2 trials (excluding the ~10% fractals in Type 2 trials that were sequence violations, and the non-sequence-violating fractals that were used to calculate the violation index). This compared neural responses for predictable versus unpredicted familiar objects. We subtracted 0.5 from the AUC, so that values higher than 0 indicated that the responses were higher for unexpected fractals versus expected fractals, and multiplied by 2 so that the range of the index was [-1, 1]. The significance of this index was tested by a rank sum test (threshold: $p < 0.01$). To further eliminate the effect of recency, we performed a 1-way ANOVA analysis (MATLAB) to measure the effect on each neuron's firing rate of whether the fractals occurred within the same trial (recent) or a previous trial (nonrecent), then subtracted the effect of recency from each neuron's responses before repeating the above ROC analysis.

The object recency index was quantified using Type 3 trials. We categorized each fractal's presentation based on whether the most recent presentation of the same fractal had occurred within the same trial (recent) or a previous trial (nonrecent). The recency sensitivity index of each neuron was quantified by AUC of ROC comparing responses for nonrecent versus recent objects. We subtracted 0.5 from the results, so that values higher than 0 indicated that the neuron had higher firing rate to nonrecent fractals than recent fractals, and multiplied by 2 so that the range of the index was [-1, 1]. For this analysis we only used object responses during the 2nd and 3rd position in the Type 3 trial sequence (so that it was possible for the object to be either recent or nonrecent). To remove sequence position effects, we subsampled the data before performing ROC analysis so that there were an equal number of recent and not recent objects at each sequence position (maximizing the contrast between conditions whenever possible by choosing the subset of nonrecent objects that were 'least recent', i.e. which had the longest time duration since their last presentation). To further eliminate the effects of sequence position and object selectivity, above and beyond the position matching procedure described above, we performed a 2-way ANOVA analysis (MATLAB) on position and object identity, then subtracted the effect of position and object selectivity from each neuron's responses before performing the above ROC analysis. The significance of this index was tested by a rank sum test (threshold: $p < 0.01$).

The sequence violation index was measured using the sequence violation trials described above. We calculated the AUCs of ROC of the neuron's firing rate to the familiar sequence-violating fractal versus the familiar non-sequence-violating fractal in the 2nd place and 3rd place respectively. We then averaged these two AUCs, and subtracted 0.5 such that numbers above 0 indicated that the neuron had higher firing rate to the sequence violated fractals than the normal fractals, and multiplied the result by 2 so that the range of the index was [-1, 1]. The significance of this index was tested by a permutation test (threshold: $p < 0.01$).

In the reward information viewing procedure, the reward value index quantified sensitivity to changes in reward value signaled by visual objects, and was quantified by an AUC of ROC that compared neuronal responses to the 100% big reward versus 0% big

reward trials (pooling informative and non-informative trials) in the last 500 ms epoch before the reward was delivered. We then subtracted 0.5 from the result of the ROC analysis such that values higher than 0 indicated that the neuron had a higher firing rate to higher reward cue than lower reward cue, and multiplied the result by 2 so that the range of the index was [-1, 1]. The significance of this index was tested by a rank sum test (threshold: $p < 0.01$).

Also in the reward information viewing procedure, the information anticipation index was adapted from the informative cue anticipation index used previously to measure how strongly a neuron anticipated the receipt of informative visual cues to resolve uncertainty about upcoming rewards.^{39,40} It was defined as the difference between the magnitudes of neuronal uncertainty signals during informative versus non-informative trials, where the uncertainty signal was defined as the AUC of ROC comparing neural activity on trials where Cue1 indicated an uncertain reward outcome (50% big) vs. a certain reward outcome (either 100% big or 0% big) in the last 500 ms epoch before the onset of Cue2. In essence, this index measured how strongly a neuron anticipated information to resolve uncertainty.^{39,40} The range of the index is [-1, 1]. The significance of this index was tested by a permutation test (threshold: $p < 0.01$).

Normalization of firing rate in the learning analysis

We z-scored each neuron's firing rates by the mean and standard deviation of the firing rates from all types of trials, and then averaged the z-scored firing rates to always novel fractals, familiar fractals, repeated novel fractals on day 1, and repeated novel fractals on days 2+, separately for each presentation within the current day. Then, for each separate presentation number in the session, we rescaled the firing rates so that the averaged normalized firing rate was 0 for always familiar fractals and 1 for novel fractals. The error bars of the normalized firing rate for repeated novel fractals were the standard errors of the mean (computed using bootstrapping, $n = 10000$ bootstraps). This analysis controls for repetition suppression because activity for repeating novel fractals is normalized to be relative to activity for always familiar fractals, and both of these sets of fractals were repeated over the course of the session in exactly analogous manners.

Learning rate analysis

The learning rate at the n th presentation in Figure 5B lower panel was calculated as follows:

$$\alpha(n) = \frac{R(n) - R(n+1)}{R(n)}$$

Where $R(k)$ in the equation is the population average normalized firing rate in response to the k -th presentation of the fractal during a session. We calculated the learning rate separately for 1st day fractals and 2nd+ day fractals. We then smoothed the learning rate using a 3-appearance bin. The error bars in Figure 6B were the bootstrap standard error of the mean ($n = 10000$ bootstraps).

Within day learning index

For each novelty-excited neuron, we compared its object responses during the first 5 and the last 5 presentations of the repeated novel fractals (Figure 1). To do this, we needed to quantify the strength of responses to the repeated novel fractals relative to responses to the always novel fractals and the familiar fractals. To accomplish this, we used a classifier to estimate the approximate posterior probability that each of these responses was evoked by an always novel fractal, given an equal prior probability of it being evoked by either an always novel fractal or a familiar fractal. To classify the firing rates to repeated novel fractals, the classifier used the equation:

$$\text{classifier}(R) = \frac{1}{\left(1 + \exp\left(\frac{a \cdot (R - b)}{\sigma^2}\right)\right)}$$

$$a = N - F$$

$$b = \frac{N + F}{2}$$

Where R is the firing rate to the repeated novel fractal, N is the mean firing rate to always novel fractals, F is the mean firing rate to familiar fractals, and σ^2 is the residual variance of the firing rate to novel and familiar fractals. All of these firing rates are the non-normalized firing rates from the individual neuron (in spikes per second) with the effect of sequence position being subtracted.

This classifier gives a result in [0, 1]. This can be interpreted as the posterior probability of the response being generated from a novel fractal, if a neuron's firing rates to novel and familiar fractals are Gaussian distributions with different means but the same variance, and both types of fractals are equally likely to have been presented. The within day learning index was defined as the difference between the mean of classification results of the repeated novel fractals at the start of day 1 vs. the end of day 1. The range of this index is [-1, 1]. Note that this analysis controls for repetition suppression because activity for repeating novel fractals is classified relative to activity for always familiar fractals, and both of these sets of fractals were repeated over the course of the session in exactly analogous manners.

Across day forgetting index

We used the same classifier as the within day learning index. The across day forgetting index was defined as the difference between the mean of classification results of repeating novel fractals at the beginning of the second and subsequent days vs. at the end of the first day. In the calculation, non-overlapping sets of fractals at the end of the first day were used in the calculation of within day learning index and across day forgetting index, such that the two measurements were statistically independent. The range of this index is $[-1, 1]$. Significance was assessed with a rank-sum test ($p < 0.05$). For comparison of brain areas' learning and forgetting indices (Figure 7C) we included brain areas with at least $n=20$ novelty excited neurons.

Control for Figure 7B

We controlled for session-to-session variability in learning, which might contribute to the correlation of within day learning index and across day forgetting index. In other words, it could be that within every single session all neurons learn and forget at the same rate as each other, but some sessions are 'fast' and other sessions are 'slow'. If so, the apparent differences in learning speeds across neurons could arise from differences in learning across sessions, not neurons. To control for this possibility, we used the following analysis. For each day, if the recording session had ≥ 5 novelty-excited neurons, the session was included. For each session we calculated the averaged within day learning index over all of these neurons and then subtracted it from each of these neuron's individual within day learning indices. We did the analogous procedure for the across day forgetting index. Lastly, we calculated the correlation of the subtracted indices.

Pupil analysis

Pupil diameter was obtained with an infrared video camera (Eyelink, SR Research). To quantify the pupil's response to novel, surprising, and nonrecent fractals (Figure 2A), we used the following procedure. First, we z-scored the pupil diameter on a trial-by-trial basis (time window from the start of the first fractal until 250ms after the third fractal disappeared). Next, for each fractal within the trial, we subtracted the baseline z-scored pupil response (response in the time window $[-80, 20]$ ms relative to fractal onset). We then averaged the pupil response in the time window $[0, 500]$ ms relative to fractal onset. Lastly, we calculated the same novelty, sensory surprise, and recency indices as we used for the neurons and then multiplied by -1 , such that the index was positive if the pupil contracted more to novel/surprising/non-recent objects.

Correlation analyses

In Figure 3A and supplemental information, the novelty responsive neuron group contained all novelty responsive neurons. In order to combine the results of novelty excited neurons and novelty inhibited neurons together, we flipped the signs of the all the indices of neurons whose novelty index is negative, while the indices of neurons whose novelty index is positive remained unchanged. In supplemental information, all indices of neurons were in their original signs. In Figure 3C and supplemental information, the bar plots were generated by binning the novelty index (x axis) into three parts, $[0, 1/6]$, $[1/6, 1/3]$, $[1/3, 1/2]$, and we calculated the mean and the standard error of the mean of the indices in y axis of the neurons in each bin. For the linear fitting we used least squares regression. For all correlation analysis, we used Spearman's rank correlation unless stated otherwise.

Classifier analyses

In Figure 3B and supplemental information we used the activity of all neurons to train and test two support vector machine (SVM) classifiers. One classifier was trained to decode sensory surprise and then was tested to determine whether it could be used to decode novelty. The other classifier was trained to decode recency and then tested to decode novelty. The training set for sensory surprise was the combination of sensory-surprising fractals (labeled as 1, they were the familiar fractals in the third position in Type 3 trials) and non-sensory-surprising fractals (labeled as 0, they were the familiar fractals in the third position in Type 2 trials). The training set for recency was the combination of non-recent fractals (labeled as 1, the fractals that had occurred in the previous trial in Type 3 trials) and recent fractals (labeled as 0, the fractals that had occurred within the same trial in Type 3 trials). The test set for the two classifiers was the same. They included novel fractals (labeled as 1, novel fractals in Type 1 trials) vs. familiar fractals (labeled as 0, familiar fractals in the second position in Type 2 trials). To avoid introducing base rate biases into the classifier, in both training and testing set, the numbers of fractals with labels 1 and 0 were balanced by subsampling. We applied this classifier analysis separately for each session, computed the percentage of objects that were classified correctly, and then averaged this percentage across sessions.

Cross-validation

For activity plots in supplemental information, we first separated the sessions into even trials and odd trials. Then we calculated the relevant indices using odd trials and used this to select neural activity from the even trials for those neurons whose indices in the odd trials were significant ($p < 0.01$) and excited ($\text{index} > 0$) or inhibited ($\text{index} < 0$). Also, we calculated the indices using even trials and used this to select neural activity from the odd trials of the neurons whose indices in the even trials were significant ($p < 0.01$) and excited ($\text{index} > 0$) or inhibited ($\text{index} < 0$). This ensured that the analysis was cross-validated, i.e. each piece of data from a neuron was selected to be used for this analysis on the basis of a separate, independent set of data from the same neuron. Finally, we plotted the average z-scored activity from the selected odd and/or even trials of the neurons. (If an individual neuron's odd and even trials were both selected, then both were contributed to this analysis.). All PSTHs were smoothed by a Gaussian kernel ($SD = 50\text{ms}$). The

p values in the PSTHs plots were rank-sum tests of the average of the two PSTHs in the target window ([0, 500] ms relative to the onset of fractals in object viewing procedure.)

Noise correlation analysis

In each session, we calculated the noise correlation (Pearson's correlation) for each pair of novelty responsive neurons responding to the novel fractals in Type 1 trials. We averaged the correlations across all pairs within the session, and then averaged across sessions. We did the same process on familiar fractals in Type 2 trials in the second position in the object sequence. We also did the same calculations using non-novelty responsive neurons.

Noise variance analysis

This analysis only included sessions with at least 5 novelty responsive neurons. In each session we defined an n -dimensional space where each dimension was the firing rate of one of the n novelty responsive neurons, and hence the response to each individual fractal presentation could be represented as a point in that space. We defined the novelty axis as a unit vector pointing from the mean of the points representing familiar fractal presentations (fractal presentations in the second position in the sequence in Type 2 trials) to the mean of the points representing novel fractal presentations (fractal presentations in the second position in the sequence in Type 1 trials). We defined random axes as unit vectors drawn randomly from a uniform distribution on the unit sphere. We then computed the ratio of the mean neural response variance projected onto the novelty axis vs. random axes, as follows. We randomly chose 5 individual fractal presentations to represent each of the following three conditions. Condition 1: 5 different novel fractals (from the second position in Type 1 trials). Condition 2: 5 individual presentations of different familiar fractals (from the second position in Type 3 trials). Condition 3: 5 repeated presentations of the same familiar fractal (from the second position in Type 3 trials, using only the remaining familiar fractal from Type 3 trials that was not included in Condition 2). We also randomly chose one random axis. For each condition, we then computed the variance of its 5 individual neural responses when they were projected onto the novelty axis, and when projected onto the random axis. We repeated this process 10,000 times, using different random selections of individual fractal presentations for each condition and a different random axis. We then computed the ratio of response variances for each condition as the mean of the 10,000 variances along the novelty axis divided by the mean of the 10,000 variances along the random axes. This produced one response variance ratio for each of the three conditions in each session. We then averaged these ratios within each condition over sessions, and tested the difference between the conditions using signed-rank tests.

Stability of object selectivity across sessions

We tested whether object selectivity of single neurons changed during novelty-familiarity transformations. In each session, we divided the repeating novel fractal presentations into three groups chronologically, and used the early group (start of the session) and the last group (end of the session) separately to measure object selectivity for each neuron. To obtain an object selectivity index we performed a 2-way ANOVA analysis on sequence position and object identity, and obtained a measure of variance explained by object identity (Var_{id}), variance explained by sequence position ($Var_{position}$) and residual variance (Var_{res}).

$$object\ selectivity\ index = \frac{Var_{id}}{Var_{id} + Var_{res}}$$

In novelty-responsive neurons, we found that there was no significant difference in their object selectivity between the start (early group) and the end of the sessions (last group) ($p = 0.24$, signed-rank test).

Hierarchical clustering of brain areas

We performed hierarchical clustering of brain areas based on the strength of their sensory surprise and recency effects relative to their novelty effects, using the following procedure. First, for each neuron we converted its novelty, sensory surprise, and recency indexes into unsigned "absolute" indexes to represent the overall strength of its coding, by multiplying each index by -1 if it had a negative sign while leaving it unchanged if it had a positive sign. Then, for each brain area, we computed the mean of each these three absolute indexes across its neurons. Finally, in order to measure sensory surprise and recency relative to novelty, we normalized the mean absolute sensory surprise and recency indexes for each area by dividing them by that area's mean absolute novelty index. Thus each area was represented as a point in a two dimensional space, defined by its normalized mean absolute indexes for coding of sensory surprise and recency. We then used hierarchical clustering to cluster the areas based on their Euclidean distance in that space and using the unweighted pair group method with arithmetic mean (UPGMA).

Current Biology, Volume 32

Supplemental Information

**Surprise and recency in novelty
detection in the primate brain**

Kaining Zhang, Ethan S. Bromberg-Martin, Fatih Sogukpinar, Kim Kocher, and Ilya E. Monosov

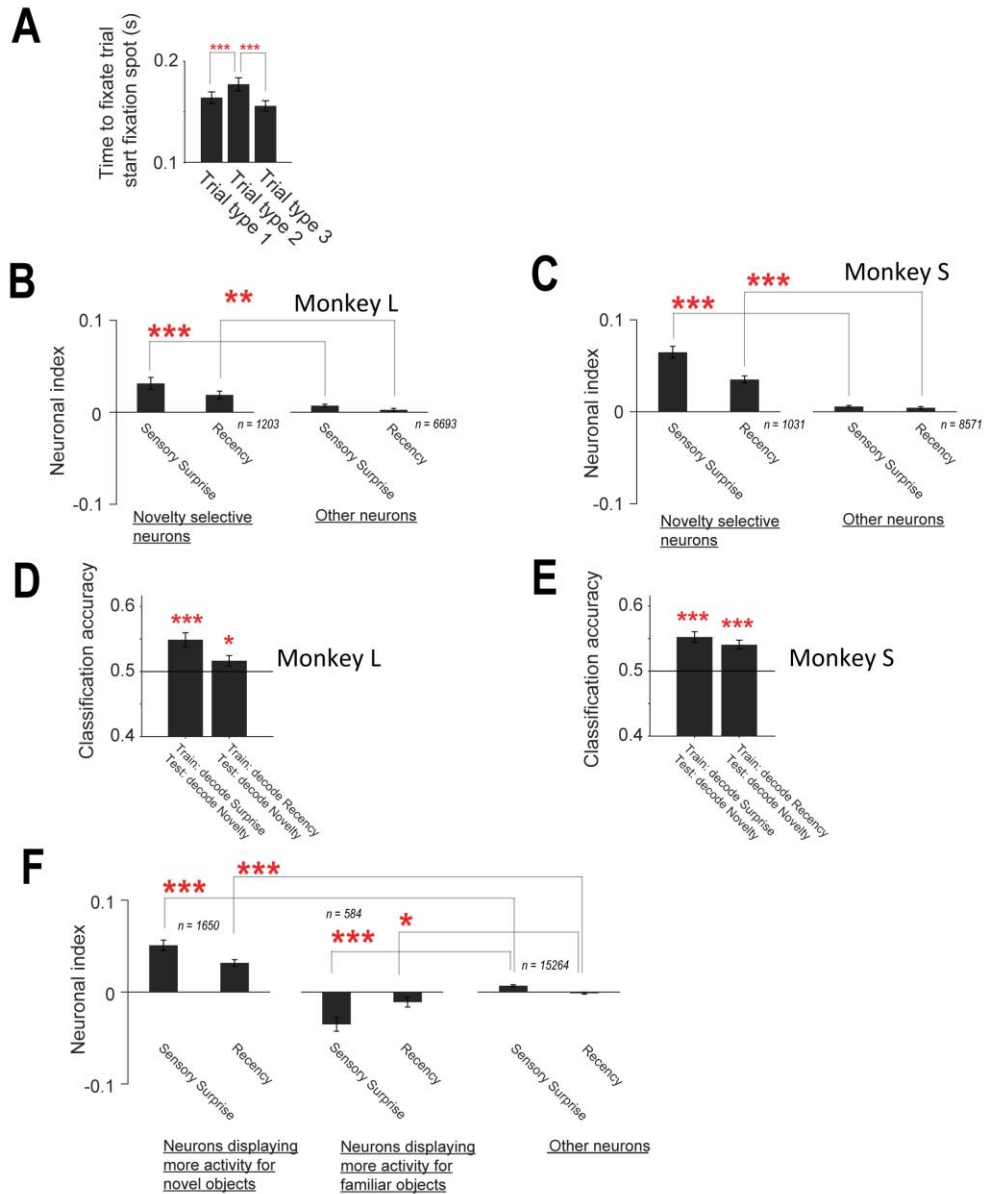


Figure S1. Trial start related behavioral analyses and neural results for two monkeys, separately. Related to Figures 1-3. (A) Monkeys' reaction times are different for the fixation dots predicting the first three trial types. **(B-E)** In both monkeys, novelty neurons displayed strong coding of sensory surprise and recency. The figure format is the same as in Figure 3. **(F)** Novelty neurons in Figure 3A shown separately for novelty-excited (higher activity for novel objects - left two bars) and novelty-inhibited (higher activity for familiar objects - middle two bars) groups. Other neurons are shown on the right (same as Figure 3). The figure format is the same as in Figure 3.

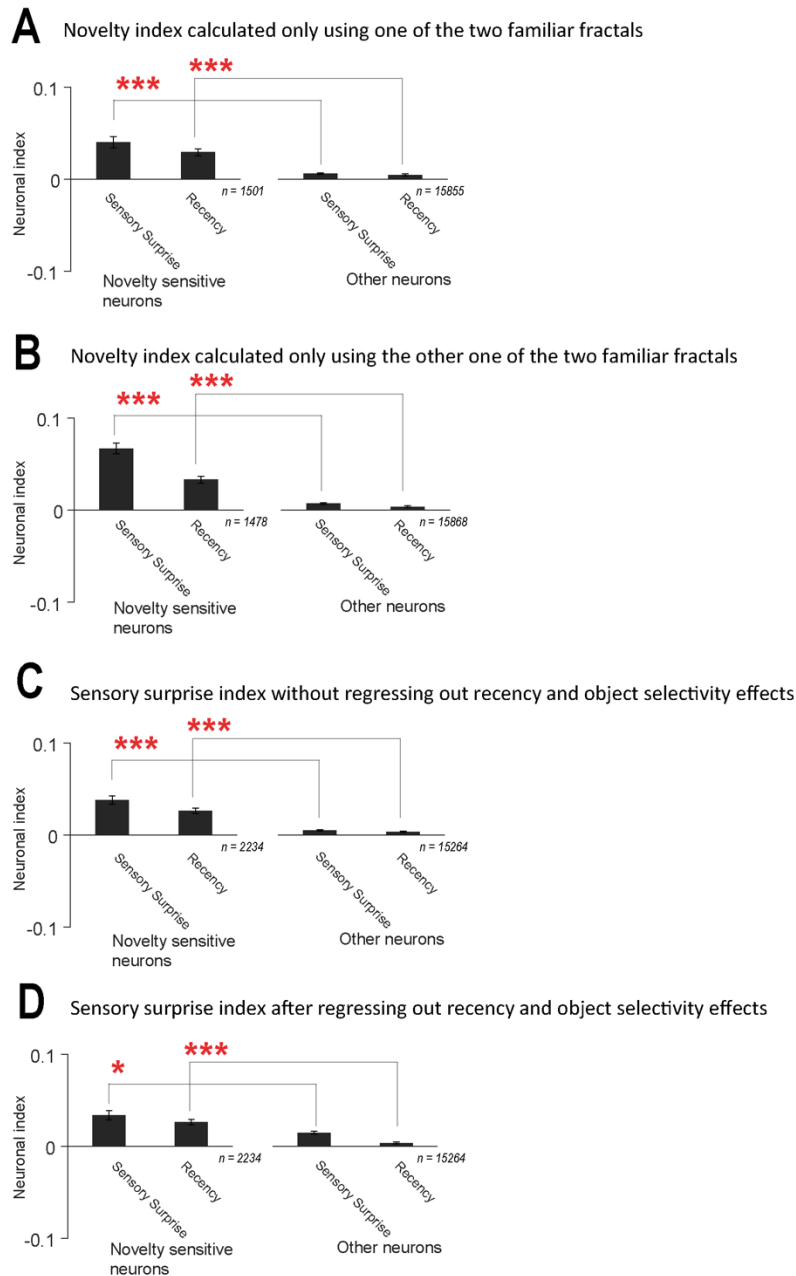


Figure S2. Supplemental analyses for novelty and surprise indices. Related to Figure 3. Correlation analysis as in Figure 3A, but using alternative methods to calculate the novelty index and sensory surprise index as controls. **(A)** We calculated the novelty index only using one of the two familiar fractals in trial type 2 at the second position in the sequence. The sensory surprise index and recency index are very similar to Figure 3. **(B)** We calculated the novelty index only using the other one of the two familiar fractals in trial type 2 at the second position in the sequence. The sensory surprise index and recency index are again very similar to Figure 3. **(C)** We calculated the sensory surprise index using the raw neural firing rates without regressing out recency and object selectivity effects. **(D)** We calculated the sensory surprise index after

regressing out recency and object selectivity effects from each neuron's firing rates (STAR Methods). In addition, the correlation coefficient of the novelty index and sensory surprise index in novelty excited neurons is 0.078 ($p < 0.01$), 0.071 ($p < 0.05$), 0.108 ($p < 0.001$), 0.064 ($p < 0.01$), respectively in the four cases, and the correlation coefficient of the novelty index and recency index in novelty excited neurons is 0.117 ($p < 0.001$), 0.038 ($p = 0.20$), 0.114 ($p < 0.001$), 0.114 ($p < 0.001$), respectively in the four cases.

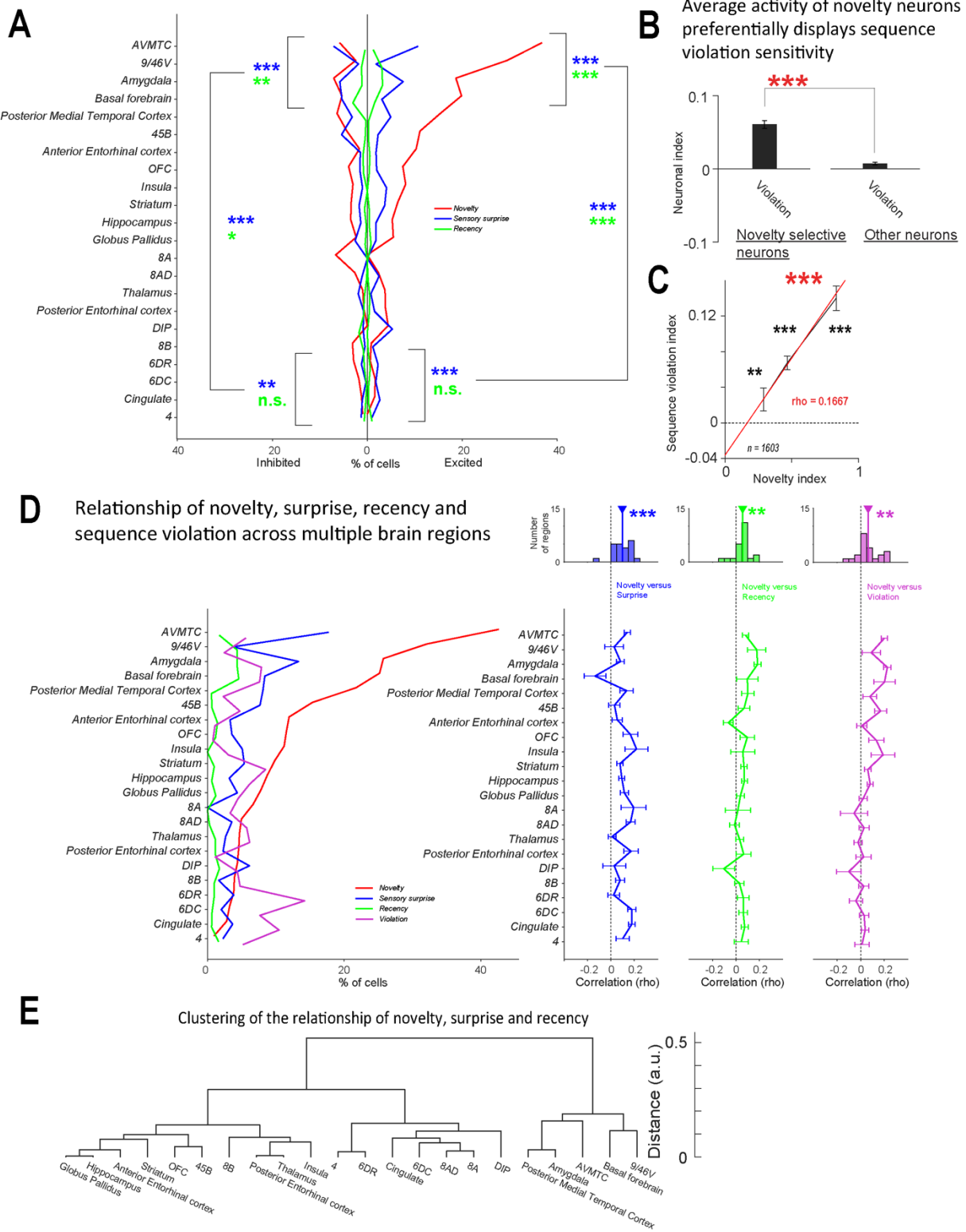


Figure S3. Novelty-excited and inhibited neurons' relationship with surprise and recency across the brain, and sequence violation coding across the brain. Related to Figure 4. (A)

We separated the neurons in figure 3C into novelty-excited, novelty-inhibited, sensory surprise-excited, sensory surprise-inhibited, recency-excited and recency-inhibited neurons. Data to the left of 0 are for inhibited neurons, and to the right of 0 are for excited neurons. Novelty, sensory surprise, and recency are indicated by red, blue, and green. Here by excited we mean higher activity, and by inhibited we mean lower activity; for example, a novelty inhibited neuron had lower firing rate for novel than familiar objects (STAR Methods). **(B-D)** Relationship of sequence violation and novelty coding. **(B)** The mean sequence violation index in all novelty responsive neurons is significantly higher than in all other neurons. **(C)** Within novelty-excited neurons, the magnitude of novelty sensitivity was correlated with the magnitude of their sensitivity to sequence violations. The figure format is the same as in Figure 3. **(D)** The distribution of neurons coding sequence violation by brain areas is distinct from novelty neurons (**left**, magenta line), but in the brain areas which had a high proportion of novelty neurons, the coding of novelty and sequence violation are correlated (**right**, magenta). Error bars indicate SE obtained through a bootstrapping procedure. The distribution of the correlations from brain areas is centered higher than 0 (signed-rank test, *, **, ***, indicate $p < 0.05$, 0.01, 0.001). **(E)** Areas can be clustered in many ways. Here the areas are clustered by their average recency and sensory surprise sensitivities (defined as in Figure 2) relative to their average novelty sensitivity (STAR Methods).

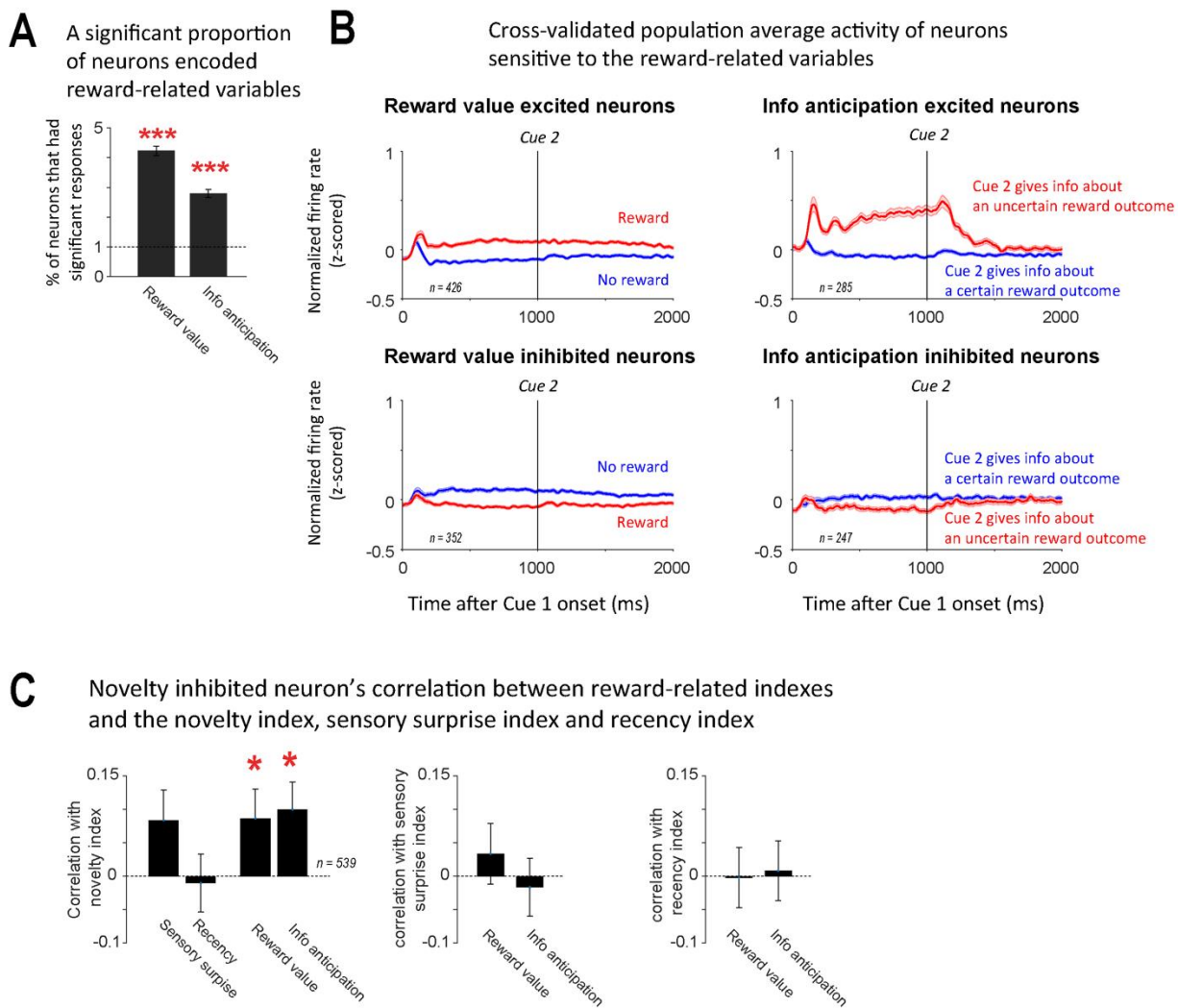


Figure S4. Supplemental analyses of reward information viewing procedure. Related to Figure 5. (A) Percentage of neurons significantly encoding reward value and information anticipation. Chance is indicated by the dotted line. (B) Cross-validated population average PSTHs of neurons encoding reward value (left) or information anticipation (right). Each neuron's activity was normalized by z-scoring before being averaged. (C) (left) Novelty-inhibited neurons' novelty sensitivity correlated with their sensitivity to reward value and information anticipation (right two bars), but did not significantly correlate with their sensitivity to sensory surprise and recency (left two bars). *, **, ***, indicate $p < 0.05$, 0.01 , 0.001 . The results of these comparisons are: novelty and reward value, $p=0.045$, novelty and information anticipation, $p=0.02$, novelty and sensory surprise, $p=0.052$, novelty and recency, $p=0.81$, Spearman's rank correlation). This implies that novelty-inhibited neurons are functionally distinct from novelty-excited neurons. (middle, right) Novelty-inhibited neurons' sensitivity to sensory surprise and recency was not significantly correlated with the magnitude of their sensitivity to reward value and information anticipation.

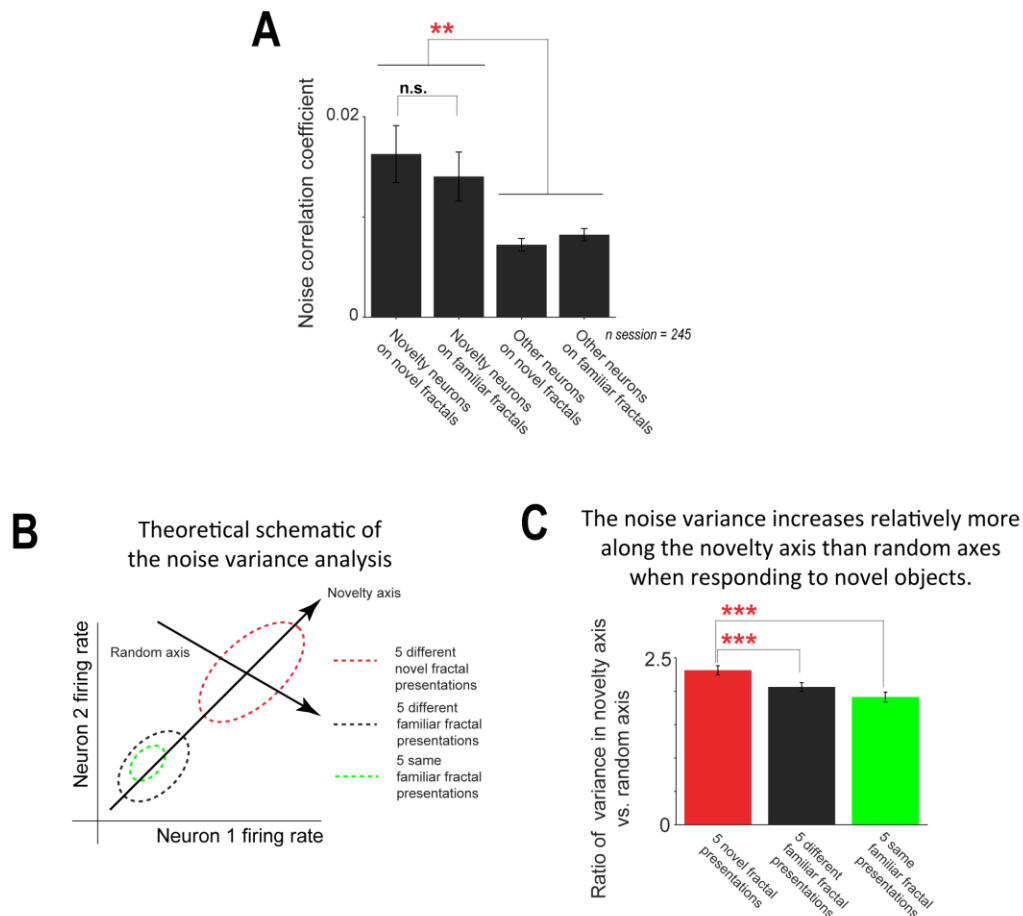
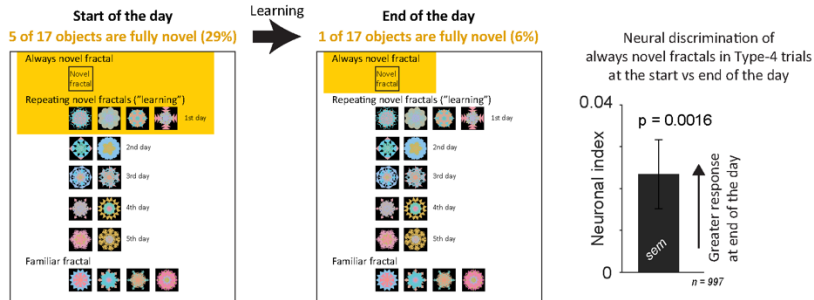


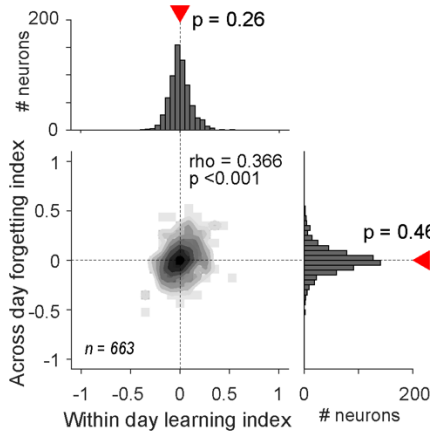
Figure S5. Common origins of novelty responses. Related to Figures 2-5. (A) Noise correlation analysis. The bars from left to right represent the mean noise correlations for the following conditions: Novelty responsive neurons' noise correlation during responses to novel fractals; novelty responsive neurons' noise correlation during responses to familiar fractals; other neurons' noise correlation during responses to novel fractals, and other neurons' noise correlation during responses to familiar fractals. Asterisks (same format as other figures) indicate significance of a comparison between novelty responsive neurons vs. other neurons comparing mean noise correlations pooled over all fractals. **(B)** Noise variance analysis. We tested if novelty responsive ensembles responded to the novel fractals in a manner consistent with novel fractals having different degrees of novelty – for example, as a result of some novel fractals being perceived as more or less novel/familiar. Specifically, we defined the ensemble response to each individual object presentation as a point in an N-dimensional firing rate space (with each dimension corresponding to the firing rate of a specific neuron, including only novelty responsive neurons). Then, using 5 individual object presentations, we computed the variance of the ensemble responses along the novelty coding axis and a random axis, bootstrapped the mean, and calculated their ratio (STAR Methods). This was done for three sets of object presentations: 5 different novel fractals, 5 different familiar fractals, and 5 presentations of the

same familiar fractal (red, black, and green circles in theoretical schematic in B; left, middle, and right bars in C). (C) The results indicated that the variance of the neural responses to novel fractals, compared to familiar fractals, was expanded relatively more along the novelty axis than the other random axes ($p < 0.0001$, signed-rank tests). This may suggest that neural systems for novelty detection can have shared response variance, effectively treating some novel objects as 'more novel' and others as 'less novel'.

A Novelty excited neurons' activity is consistent with increasing surprise at the presence of novel fractals as they become less commonly encountered during Type-4 trials due to learning



B Within-day learning predicts across-day forgetting in single neurons after controlling for session-to-session variation in learning and forgetting



C Heterogeneity in average learning and forgetting across brain regions

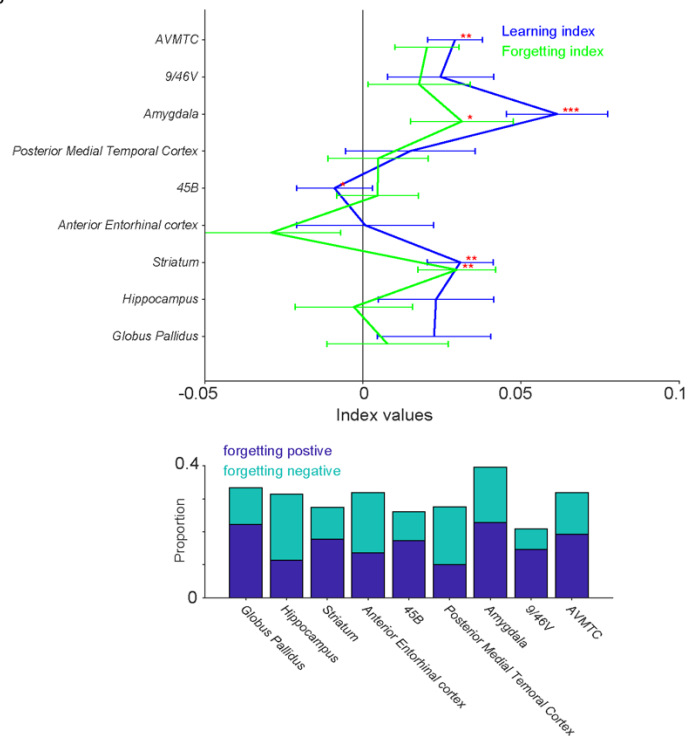


Figure S6. Supplemental analyses of learning and forgetting. Related to Figure 6. (A) In Type-4 trials, as animals learned to become familiar with the repeating novel fractals after repeated exposure, this caused the probability of encountering never-before-seen novel fractals to become much less common (Left panel; start of session: 5/17; end of session: 1/17). Hence, if animals tracked this reduction in the probability of encountering completely novel objects, they might treat the presentation of the always novel objects as increasingly 'surprising'. Furthermore, we hypothesized that novelty responsive neurons might be sensitive to this form of surprise (i.e. surprise induced by a novel object when animals predict that a novel object has a

low probability of appearing), given our finding that many of these neurons respond to a different form of surprise (i.e. sensory surprise induced when a specific familiar object has a low probability of appearing; Figure 3). Indeed, the activity of novelty-excited neurons reflected this additional novelty-related surprise by increasing their responses to the always novel objects towards the end of the session. We introduced an index to quantify the effect. Both Type 1 trials and Type 4 trials had novel fractals. In Type 1 trials the percentage of novel fractal was a constant, so we used it to control for any possible drift over time in neural response patterns. The index was calculated as the AUC of the ROC of the neuron's firing rates to the first 5 presentations vs. last 5 presentations of always novel fractals in Type 4 trials minus the AUC of the ROC of the neuron's firing rate to the first 5 presentations vs. last 5 presentations of novel fractals in Type 1 trials. The bar plot shows that the mean index was significantly greater than 0. **(B)** Importantly, the correlation between learning and forgetting indexes reflected differences in neural learning, and did not result from any possible session-to-session variations in animal learning or behavior. For example, hypothetically, even if all neurons learned in lock-step with each other within each individual session, if the animal learned fast in some sessions and slow in other sessions, this would produce a dataset where some neurons had fast learning curves and other neurons had slow learning curves. To control for this possibility, we repeated the analysis after subtracting the mean of the indices for each session's data from all neurons recorded during that session (STAR Methods). The results were very similar to Figure 7. Note that the marginal histograms are no longer significant because the indexes were mean-subtracted within each session, and hence the mean indexes must be equal to 0. **(C-top)** Data of Figure 7C with SEM. Solid lines are the means of the within-day learning index and across-day forgetting index. Error bars indicate standard error of the mean (SEM). **(C-bottom)** Proportions of cells with significant negative or positive forgetting indices (threshold: $p=0.05$) are indicated below.

Monkey L	totalCell	mean(L) to AC	mean(A) to AC	mean(D) to AC	std(L)	std(A)	std(D)
AVMTC	911	13.2	-1.11	-16.8	1.98	1.45	1.84
Basal forebrain	94	6.16	0.0877	-4.63	1.06	0.309	1.03
Amygdala	684	10.8	-0.179	-9.9	2.76	1.85	1.95
Posterior Medial Temporal Cortex	150	14.9	-6.9	-16.4	0.00129	1.86	0.62
45B/8v	110	13.5	4.73	8.19	1.75	0.00084	0.866
Anterior Entorhinal cortex	503	9.4	-3.01	-16.3	1.4	1.36	0.865
Striatum	560	10.3	-2.09	-0.32	3.56	3.64	6.66
Insula	42	16.4	3.45	-0.451	0.00124	0.575	1.01
Hippocampus	833	11.9	-6.4	-11.2	2.59	3.88	2.3
Globus Pallidus	229	6.95	-2.85	-0.87	1.35	1.66	1.58
8A	56	14.9	2.99	9.21	2.34	0.537	1.19
DIP	114	9.42	-16.6	11.2	1.07	0.428	1.02
Posterior Entorhinal cortex	68	8.56	-7.47	-13.5	0.883	0.00074	1.47
8AD	185	11.7	3.92	11.1	1.42	0.763	1.58
Thalamus	373	7.21	-10.8	-0.202	1.41	2.92	2.15
8B	140	9.04	4.73	13.3	0.995	0.00074	0.914
6DR	81	8.82	4.58	17.1	1.5	0.457	1.12
6DC	283	8.26	1.74	14.4	1.45	1.29	2.79
Cingulate	726	5.92	-5.78	14.6	0.532	5.27	2.17
Area 4	2	5.69	-12	19.2	0	0	0

Monkey S	totalCell	mean(L) to AC	mean(A) to AC	mean(D) to AC	std(L)	std(A)	std(D)
AVMTC	532	14.5	-1.19	-17.2	1.66	1.47	1.39
9/46V	162	12.7	10.9	8.76	0.638	0.623	0.549
Basal forebrain	37	7.2	0.0499	-5.19	1.19	0.945	0.574
Amygdala	404	12.5	-0.787	-11.7	1.79	1.32	1.7
Posterior Medial Temporal Cortex	195	15.9	-6.06	-1.7	0.764	2.55	1.54
45B/8v	332	14	3.11	8.83	1.45	1.31	1.3
OFC	251	11.8	9.18	1.11	2.31	1.07	1.81
Anterior Entorhinal cortex	41	10	-2.15	-17.6	0.724	1.14	0.68
Striatum	944	12	-3.94	-1.88	3.5	5.1	5.11
Insula	56	14.9	-0.103	0.104	0.89	6.81	4.61
Hippocampus	766	13.8	-6.85	-12.2	2.09	2.88	2.01
Globus Pallidus	665	9.09	-3.33	-1.53	1.98	2.13	1.31
8A	34	14.4	-1.11	11.4	0.735	0.438	0.524
Posterior Entorhinal cortex	194	11.7	-7.94	-14.7	0.877	1.43	2.09
8AD	459	11.9	3.69	14.3	1.6	2	0.864
Thalamus	566	7.72	-9.5	2.78	1.31	2.01	1.98
8B	467	7.9	5.92	14.2	1.47	2.09	1.43
6DR	334	7.31	3.85	16.8	1.32	1.35	0.687
6DC	460	9.49	-0.609	16	2.4	2.2	1.31
Cingulate	411	5	7.51	13.2	0.985	3.54	1.12
Area 4	306	9.92	-8.67	17	2.94	1.65	1.27

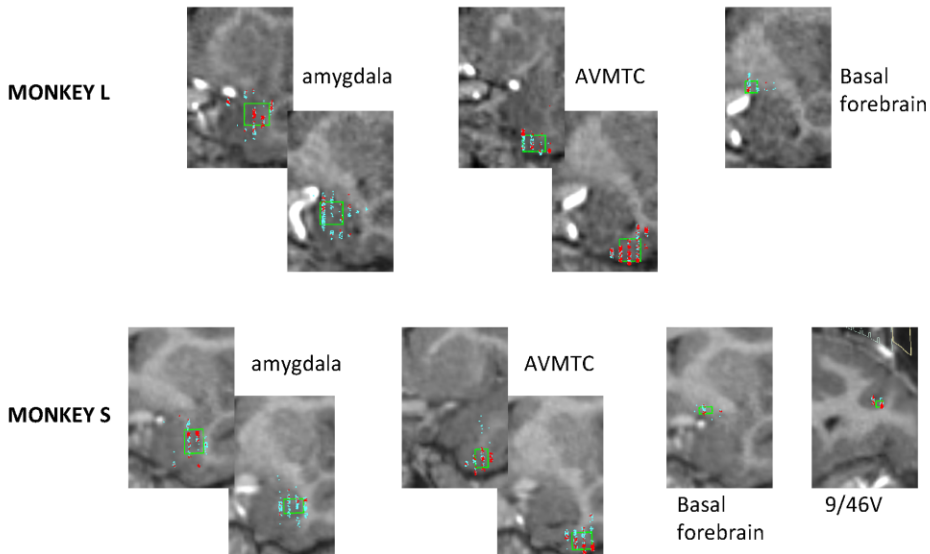


Figure S7. Recording locations. Related to Figures 1-7. (Top) Recording locations relative to the anterior commissure (AC) in each monkey. All units are in mm. Cell count: number of cells in the region. mean(L) to AC(L): mean of lateral coordinates of the cells in the region, referenced

to AC. mean(A) to AC(A) : mean of anterior coordinates of the cells in the region, referenced to AC. mean(D) to AC(D) : mean of dorsal coordinates of the cells in the region, referenced to AC. std(L), std(A), std(D) : standard deviation of lateral, anterior, and dorsal coordinates of the cells in the region. (**Bottom**) MRI images and recording sites in areas preferentially enriched (top 4) with novelty neurons. The neurons are projected onto coronal MRI slices (top: monkey L and bottom monkey S). Blue dots represent cells which do not selectively respond to novelty and red cells represent cells which do selectively respond to novelty. Green rectangle shows one standard deviation of cells' coordinates around their means in dorsal and lateral directions. Monkey L : AVMTC is shown on two planes at AP +23.4 and AP +19.6, Basal Forebrain is shown on AP + 19.5, Amygdala is shown on AP +22.2 and AP +20.4. Monkey S: AVMTC on AP +24.0 and AP +18.4, 9/46V on AP +30.3, Basal Forebrain on AP +20.1, Amygdala on AP +20.3 and AP + 19.0. AP - anterior posterior axis. Here numbers are relative to the interaural (where the center of the AC is on average between 20+ and 21+ AP).